運輸省港湾技術研究所 (25th Anniversary Issue)

港湾技術研究所報告

REPORT OF THE PORT AND HARBOUR RESEARCH INSTITUTE

MINISTRY OF TRANSPORT

VOL. 26 NO. 5 DEC. 1987

NAGASE, YOKOSUKA, JAPAN

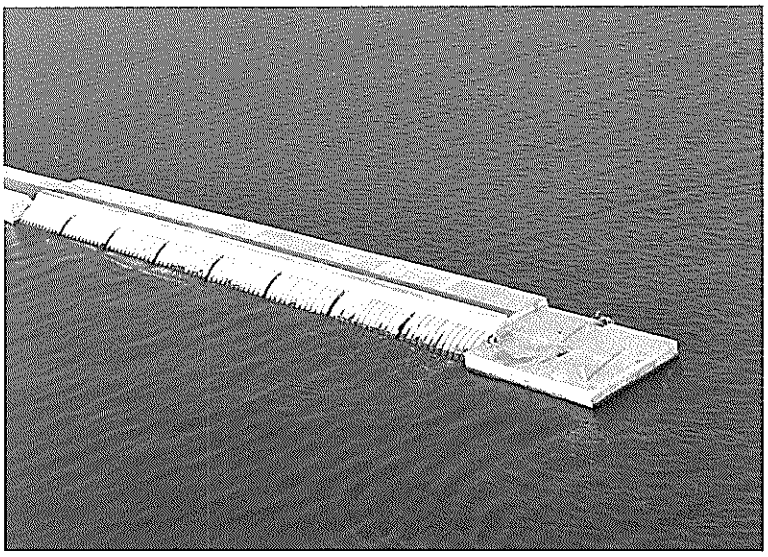

Curved Slit Caisson Breakwater

View of curved slit caisson breakwater completed in the construction at the port of Funakawa. (Courtesy of Akita Port Construction Office, the First District Port Construction Bureau, Ministry of Transport)

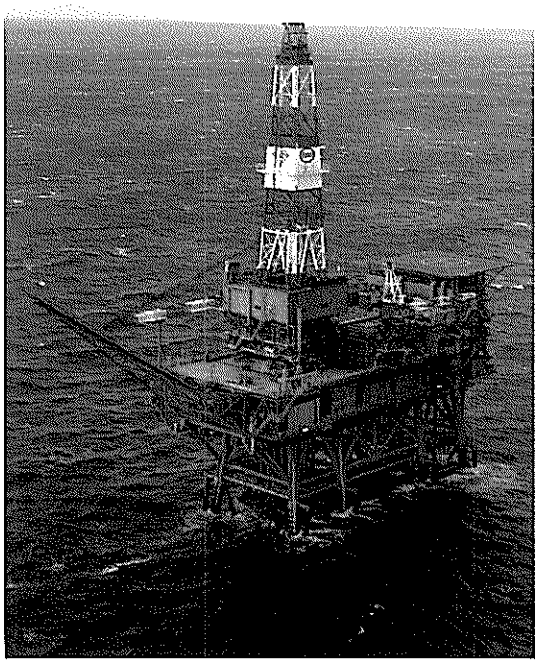

Facilities for Ocean Directional Wave Measurement

Four step type wave gauges and a two-axis directional current meter with a pressure sensor are installed on the legs of an offshore oil rig. They are operated simultaneously for detailed directional wave analysis.

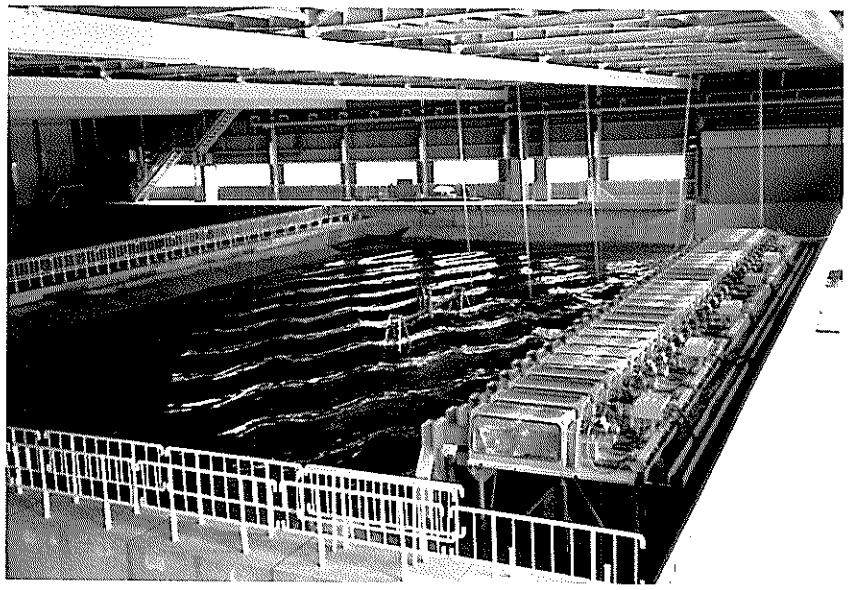

Serpent-type Wave Generator

The photograph shows the serpent-type wave generator in the short-crested wave basin and the superimposition state of two different oblique waves generated by the generator.

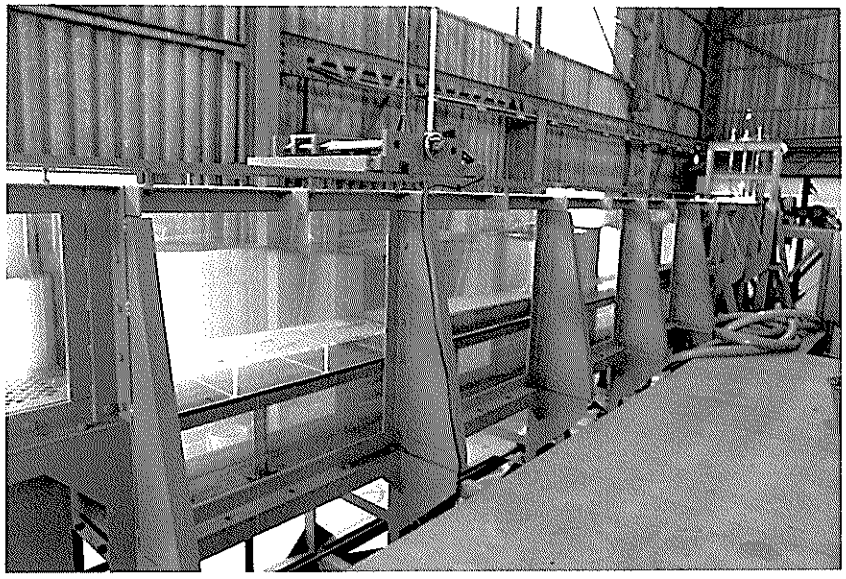

Wave-soil Tank

The experiments concerning the wave-soil interactions are conducted in this tank. The soil tank and the test section are located at the center of the tank. A movable floor is provided at the bottom of the test section and the level of the interface of mud layer and water can easily be adjusted to the level of the flume bottom.

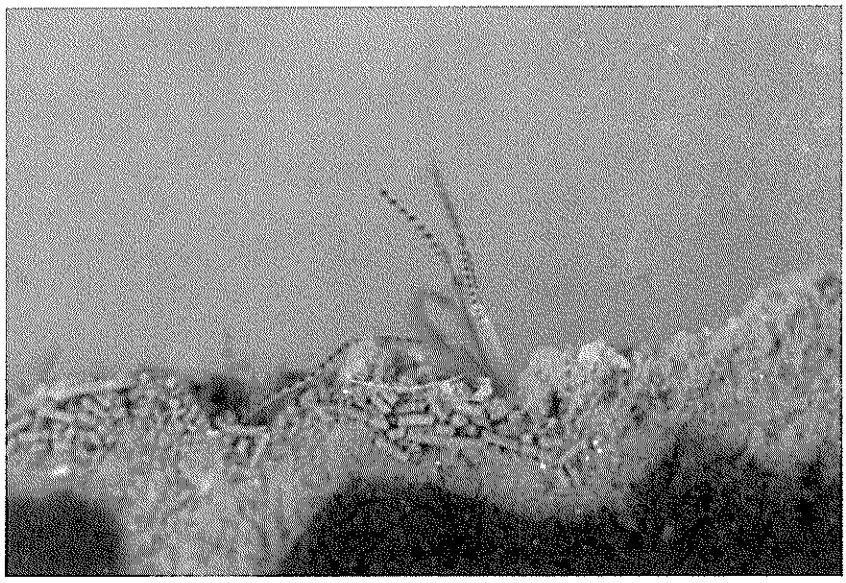

Pararionospio Pinnata

The biomass of benthos is one of the most sensitive indices to know the effect of sea-bed sediment treatments on the marine environmental improvement. The picure shows a kind of benthos, *pararionospio pinnata,* which preferentially exists in the polluted sea-bed.

Breakwater Damaged by Storm

This photograph shows a breakwater damage by a storm.
The breakwater is of the composite type with concrete caisson on a rubble mound. Two caissons were severly damaged due to the instability of a rubble mound.

Nondestructive Evaluation of Pavement

Nondestructive methods for evaluating the load carrying capacity of airport concrete pavements have been developed by using Falling Weight Deflectometer(FWD).

Seismic Damage to Gravity Quaywall

The 1983 Nipponkai-Chubu earthquake(Magnitude : 7.7)caused serious damage to port facilities in northern part of Japan. This photo shows the damage to gravity quaywall. The concrete cellular block walls were collapsed and completely submerged.

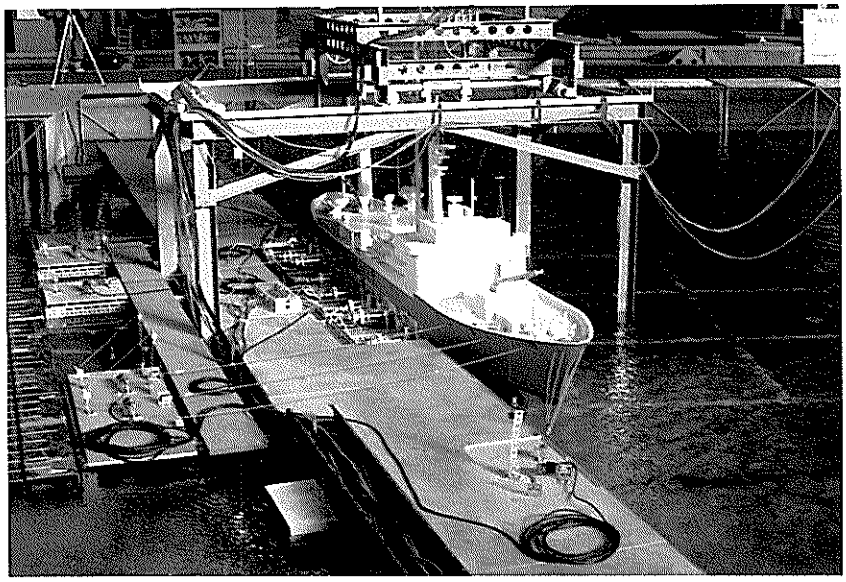

Model Experiment of Mooring Ship

Model ship is moored at a quay wall with fenders and mooring ropes subjected to gusty wind and/or irregular waves.

Vessel Congestion in Japan

As Japan is surrounded by the sea, there are many crowded water areas with various sizes and types of vessels. Arround there, many construction works were planned such as ports and harbours, off-shore airports, huge bridges and so on, so that many marine traffic observations and marine traffic simulations have been carried out.

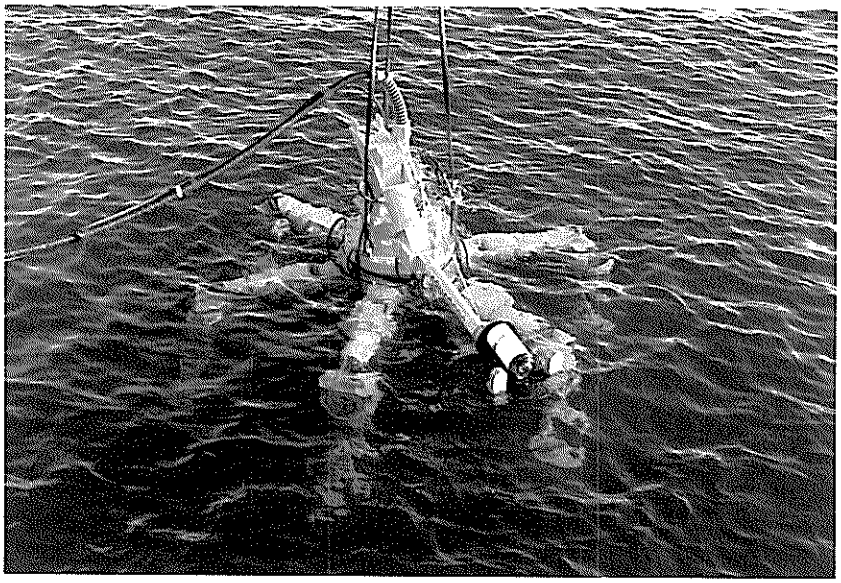

Underwater Inspection Robot

This is the six-legged articulated underwater inspection robot named "AQUAROBOT". The robot controlled by a computer can walk on uneven sea bed without making water muddy.

Foreword

The Port and Harbour Research Institute is a national laboratory under the Ministry of Transport, Japan. It is responsible for solving various engineering problems related to port and harbour projects so that governmental agencies in charge of port development can execute the projects smoothly and rationally. Its research activities also cover the studies on civil engineering facilities of air ports.

Last April we have celebrated the 25th anniversary of our institute because the present organization was established in 1962, though systematic research works on ports and harbours under the Ministry of Transport began in 1946. As an event for the celebration, we decided to publish a special edition of the Report of the Port and Harbour Research Institute, which contains full English papers only. These papers are so selected to introduce the versatility of our activities and engineering practices in Japan to overseas engineers and scientists. It is also intended to remedy to a certain extent the information gap between overseas colleagues and us.

The reader will find that our research fields cover physical oceanography, coastal and ocean engineering, geotechnical engineering, earthquake engineering, materials engineering, dredging technology and mechanical engineering, planning and systems analysis, and structural analysis. Such an expansion of the scope of research fields has been inevitable, because we are trying to cover every aspect of technical problems of ports and harbours as an integrated body.

The present volume contains eleven papers representing six research divisions of the institute. The materials introduced in these papers are not necessarily original in strict sense, as some parts have been published in Japanese in the Reports or the Technical Notes of the Port and Harbour Research Institute. Nevertheless they are all original papers in English and are given the full format accordingly. We expect that they will be referred to as usual where they deserve so.

It is my sincere wish that this special edition of the Report of the Port and Harbour Research Institute will bring overseas engineers and scientists more acquainted with our research activities and enhance the mutual cooperation for technology development related to ports and harbours.

December 1987
Yoshimi Goda
Director General

港湾技術研究所報告 (REPORT OF P. H. R. I.)
第26巻 第5号 (Vol. 26, No. 5) 1987年12月 (Dce. 1987)

目　　次 (CONTENTS)

REPORT OF THE PORT AND
HARBOUR RESEARCH INSTITUTE
Vol. 26, No. 5 (Dec. 1987)

1. Structures and Hydraulic Characteristics of Breakwaters — The State of the Art of Breakwater Design in Japan —

Katsutoshi TANIMOTO*
Shigeo TAKAHASHI**
Katsutoshi KIMURA***

Synopsis

Since the country is surrounded by rough seas, breakwaters are the fundamental harbour facilities in Japan and so occupy an important position in port and harbour engineering from both viewpoints of the design technique and the construction cost. Responding to this situation, intensive studies on the breakwaters have been carried out during a quarter of century at the PHRI. In the present paper, some recent results are reviewed because most of them have been reported in Japanese only.

The major structure type of breakwaters in Japan is a mixed type which consists of a rubble mound foundation and an upright section, while rubble mound breakwaters are presently the most common type in the world. Mixed type breakwaters of which the upright sections are covered with wave dissipating concrete blocks are also popular in Japan. In the paper, the hydraulic characteristics of those conventional breakwaters are first described including already established formulae. In particular, experimental data on the transformation of irregular waves transmitted behind a breakwater during the propagation are newly presented.

On the other hand, changes of surrounding conditions related to breakwater constructions are recently emerging. In particular, necessity of constructing breakwaters in deep and rough seas results in the marked increase of the cost, and demands the development of new economical breakwater structures. In the paper, several new breakwater structures such as sloping top caissons, multi-cellular caissons, curved slit caissons, wave power extracting caissons, trapezoidal caissons and dual cylinder caissons are introduced with the present states of their developments.

* Chief of Breakwaters Laboratory, Hydraulic Engineering Division
** Chief of Wave Power Laboratory, Hydraulic Engineering Division
*** Member of Breakwaters Laboratory, Hydraulic Engineering Division

港湾技術研究所報告
第26巻 第5号 (1987.12)

1. 防波堤の構造と水理特性
—日本における防波堤設計の現状—

谷本勝利*・高橋重雄**・木村克俊***

要　旨

波浪条件の厳しい我が国の港湾においては，防波堤は重要な基本施設であり，技術的にも工費的にも大きな比重を占めている。そのため，防波堤に関しては非常に多くの調査研究が行われておりその成果が発表されているが，そのほとんどは日本語で書かれたものであって，諸外国にあまり紹介されていない。本報告は我が国の防波堤の設計や新構造の開発について，主として港湾技術研究所における最近の成果を水工的側面からとりまとめたものである。

我が国における防波堤の主要構造様式は捨石マウンドの上にケーソンを据付けた混成堤であって，傾斜堤主体の諸外国の現状とは異なっている。また，ケーソンの前に消波ブロックを投入した形式の防波堤も多い。本報告では，まずこれらの在来形式の反射・伝達波特性や波力安定性について，既に確立されている諸公式を含めて概観した。特に，伝達波については伝播に伴うその特性の変化について新しいデータを示している。

他方，近年における防波堤建設をとりまく諸情勢の変化，特に大水深，大波浪化の趨勢は工費の著しい増大をもたらせており，より合理的で経済的な防波堤構造の開発を要請している。これに対応してこれまで行ってきた新防波堤構造の開発の現状を紹介した。取り上げた構造の主要なものは，上部斜面ケーソン，マルチセルラーケーソン，曲面スリットケーソン，波力発電ケーソン，台形ケーソン，二重円筒ケーソン等である。

* 水工部　防波堤研究室長
** 水工部　波エネルギー研究室長
*** 水工部　防波堤研究室

Contents

1. Introduction

The most common type of breakwater in the world is the rubble mound breakwater, which is the most primitive but may be the most economical type. Nevertheless, vertical breakwaters have also been constructed in some countries. In particular mixed type breakwaters, which consist of a rubble mound foundation and an upright section as shown in Fig. 1, are very popular in Japan.

Mixed type breakwaters have several advantages over rubble mound breakwaters. They are more stable, faster to construct, and less in wave transmission than rubble mound breakwaters. Because of these advantages, a large total length has been built in Japan without major mishaps for several scores of years in the past. However, the mixed type breakwaters have a disadvantage of high reflection since they have a reflective wall. Also, because the wave pressure acts on the vertical wall with almost the same phase from the top to the bottom, the resultant wave force becomes large. In very unfavourable conditions, powerful impact forces are caused by the action of breaking waves as imagined by Photo 1.

Such disadvantages of the mixed type breakwaters are emerging due to recent changes of surrounding conditions related to breakwater constructions in Japan. Wave reflection from breakwaters, which causes additional agitation, frequently becomes an important problem because a water area neighbouring to a harbour is highly utilized for fishery activities and navigation of small crafts. Also, the development of ports from natural small harbours to artificial large harbours facing the outer sea has demanded the construction of breakwaters in more rough seas. Nowadays, breakwaters having the upright section with a width of more than 20 m are not unusual and even the upright section of about 35 m in the width can be found at a few ports in the south-west islands in Japan.

In order to cope with these disadvantages, mixed type breakwaters covered with wave dissipating concrete blocks as shown in Fig. 2 have been constructed in many harbours where the water depth is relatively shallow. However, the recent trend of breakwater constructions in deep and rough seas necessitates the use of large size blocks, and another problem of the block strength has arisen lately. Moreover, the most important aspect is that the construction cost increases exponentially with the

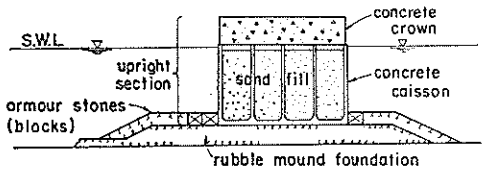

Fig. 1 Mixed Type Breakwater

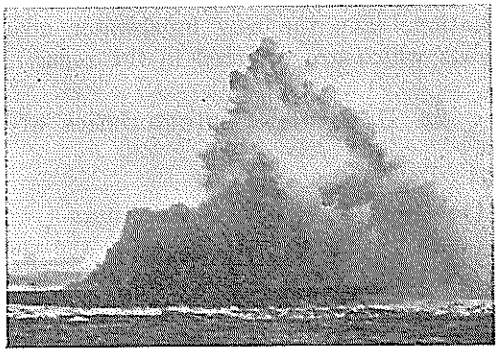

Photo 1 Wave Action on Mixed Breakwater

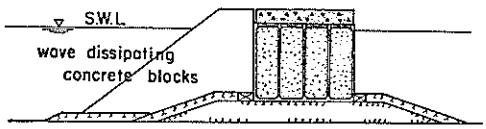

Fig. 2 Mixed Type Breakwater Covered with Wave Dissipating Concrete Blocks

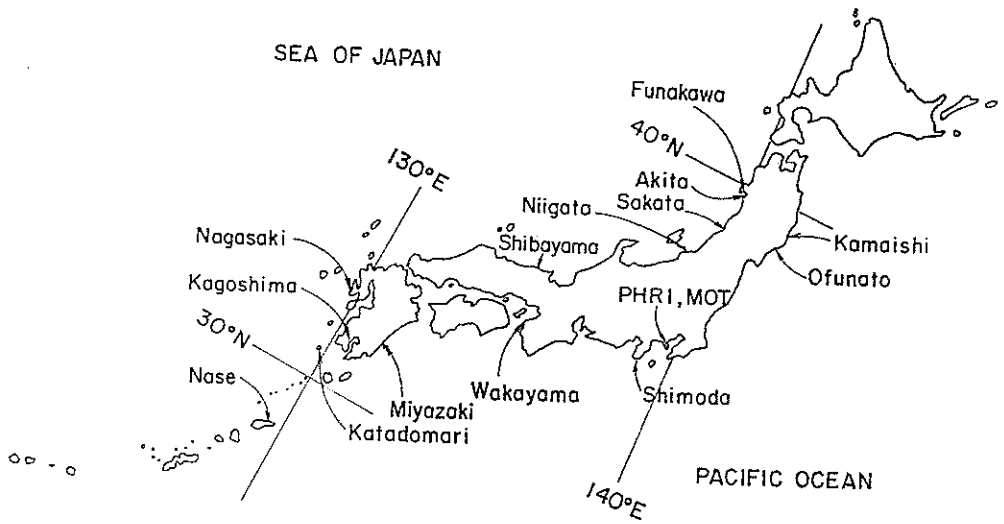

Fig. 3 Location Map of Ports Referred in the Report

construction depth, because the structure is of the semi-sloping type, and the sectional area becomes large.

Under the circumstances mentioned above, the development of new types of breakwater structures, which are suitable to the conditions of deep water and high waves, is an exciting subject in Japan, and intensive efforts are being made to develop a reasonable structure of breakwaters. In this report, the present state of these efforts is introduced together with some hydraulic aspects for both the conventional and the new breakwater structures. Figure 3 indicates the location of ports which are referred in the report.

2. Hydraulic Characteristics of Conventional Breakwaters in Japan

2.1 Definitions

(1) Cross Section of Breakwaters

As mentioned in Chapter 1, the conventional breakwater structure in Japan is the mixed type with or without wave dissipating concrete blocks in front of the upright section. Figure 4 indicates the notations to define the cross section of the breakwaters, where h is the depth, h' is the bottom depth of the upright section, d is the crest depth of the armour layer of the rubble mound foundation, h_c is the crest

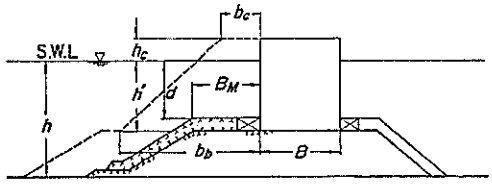

Fig. 4 Definition Sketch of Cross Section of Mixed Type Breakwater

height of the upright section, B is the width of the upright section, B_M is the berm width of the rubble mound foundation, b_c and b_b are the crest and the bottom widths of the covering section with wave dissipating concrete blocks. The crest height of the covering section with the wave dissipating concrete blocks is equal to that of the upright section.

(2) Definition of Reflection and Transmission Coefficients

When waves act on breakwaters, part of the incident wave energy is dissipated. Part of remaining energy, however, is reflected and generates reflected waves in front of the breakwaters. The rest is transmitted and yields waves transmitted behind the breakwaters. The wave reflection is sometimes problem because it makes another agitation in front of the breakwaters. On the other hand, the wave transmission is essentially important in the design of breakwaters because the most principal function of breakwaters is to prevent wave propagation behind them and so create a calm water area there.

The degrees of wave reflection and transmission are usually measured by the reflection coefficient K_R and the transmission coefficient K_T which are defined by the following relations:

$$K_R = H_R/H_I \tag{1}$$

$$K_T = H_T/H_I \tag{2}$$

where, H_I; incident wave height, H_R; reflected wave height, H_T; transmitted wave height.

All the data presented in this paper are the results of irregular wave experiments, unless otherwise mentioned. The reflection and transmission coefficients for irregular waves are defined by the ratios of the corresponding significant wave heights.

2.2 Wave Reflection

(1) Reflection Coefficient of Mixed Type Breakwaters

The reflection coefficient of mixed type breakwaters is generally high, but less than 1.0 due to the effects of rubble mound foundation and wave overtopping. In particular, it is reduced considerably when breaking waves act on the breakwaters. Figure 5 shows experimental results by two series for various wave conditions which are represented by the incident significant wave height $H_{1/3}$ and the wavelength $L_{1/3}$ corresponding to the significant wave period $T_{1/3}$. In the first series, the relative thickness of rubble mound foundation to the water depth, d/h, is changed mainly. On the other hand, the relative crest height of the upright section to the water depth, h_c/h, is changed in the second series.

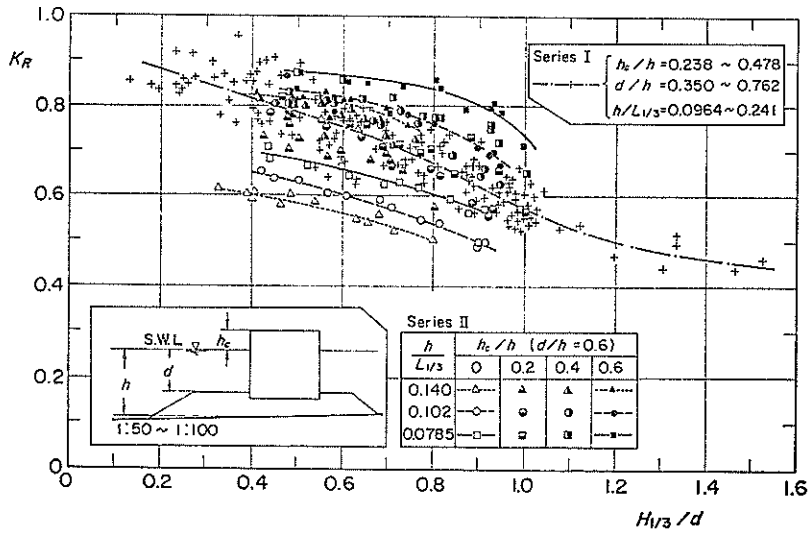

Fig. 5 Reflection Coefficients of Mixed Type Breakwaters

The abscissa in the figure is taken as the ratio of the incident significant wave height to the depth at the rubble mound foundation including the armour layer, $H_{1/3}/d$, which can be considered as a principal factor to present the degree of wave breaking. The dot-dash-line indicates the average relation of the experimental data of the series I. Other lines indicate the lower and upper limits of the data of the series II by the different conditions of the relative water depth, $h/L_{1/3}$. The results display that the reflection coefficient has the apparent tendency to decrease the value with the increase of $H_{1/3}/d$. Another important parameter is the relative crest height to the incident significant wave height, $h_c/H_{1/3}$, because it greatly controls the wave overtopping. The results of the series II display the fact, although the crest height is expressed in the dimensionless form by the water depth in the figure.

(2) Reflection Coefficient of Mixed Type Breakwaters Covered with Wave Dissipating Concrete Blocks

In order to reduce the wave reflection and wave forces, the upright section is frequently covered by wave dissipating concrete blocks. The reflection coefficient of the mixed type breakwaters covered with wave dissipating concrete blocks is greatly influenced by the relative covering width to the wavelength. Figure 6 shows the experimental results of the reflection coefficient. The symbol B_e in the figure is the equivalent covering width defined by the following relation:

$$B_e=b_0-\frac{\cot\theta}{h+h_c}\left\{\int_{-h}^{0}\frac{\cosh^2 2\pi(h+z)/L}{\cosh^2 2\pi h/L}zdz+\frac{1}{2}h_c^2\right\} \qquad (3)$$

where b_0 is the covering width at the still water level, θ is the angle of the structure slope measured from the horizontal, and z is the upward ordinate from the still water level.

The data in the figure are distinguished by the different marks for the different ranks of $B_e/L_{1/3}$ and h_c/h. The lines shows the average relation of the data specified for the rank of $0.2<h_c/h\leqq 0.4$, and values indicate the actual ranges of h_c/h and

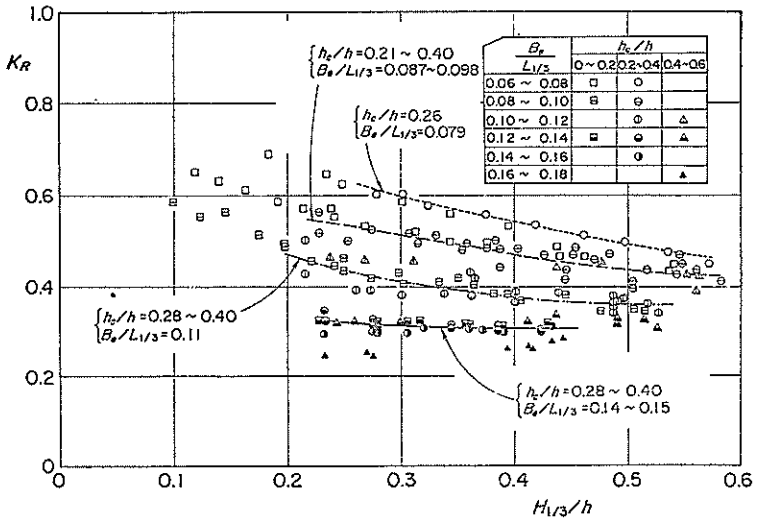

Fig. 6 Reflection Coefficients of Mixed Type Breakwaters Covered with Wave Dissipating Concrete Blocks

$B_e/L_{1/3}$. The results demonstrate that the reflection coefficient decreases in the value with the increase of $B_e/L_{1/3}$.

2.3 Wave Transmission

(1) General Expression of Transmission Coefficient

Transmitted waves are caused by transmission through the structure and by overtopping. When the transmission coefficients by both causes are denoted as K_{Tt} and K_{To}, the total transmission coefficient K_T can be expressed as

$$K_T=\{K_{Tt}^2+K_{To}^2\}^{1/2}. \tag{4}$$

Because transmitted waves by the overtopping are generated by the dropping of the water mass, they have a complicated form with high frequency components. Therefore, not only the wave height but also the wave period of transmitted waves are different from those of incident waves in general. Another interesting phenomenon is that transmitted irregular waves change characteristics such as the distributions of wave height and period as they propagate for a long distance.

(2) Transmission Coefficient of Mixed Type Breakwaters

Wave transmission of the mixed type breakwaters is mainly the result of waves generated at the lee by the impact of the fall of the overtopping water mass. Therefore, the ratio of the crest height of the breakwater to the incident wave height is the principal parameter governing the wave transmission coefficient.

Goda et al. (1969)[1] proposed the following relations of the transmission coefficient for mixed type breakwaters, based on regular wave tests:

$$\left.\begin{aligned} K_T&=\left[0.25\left\{1-\sin\frac{\pi}{2\alpha}\left(\frac{h_c}{H_I}+\beta\right)\right\}^2+0.01\left(1-\frac{h'}{h}\right)^2\right]^{1/2} \\ &\qquad ;\ \beta-\alpha<h_c/H_I<\alpha-\beta \\ K_T&=0.1\left(1-\frac{h'}{h}\right) \qquad ;\ h_c/H_I\geq\alpha-\beta \end{aligned}\right\} \tag{5}$$

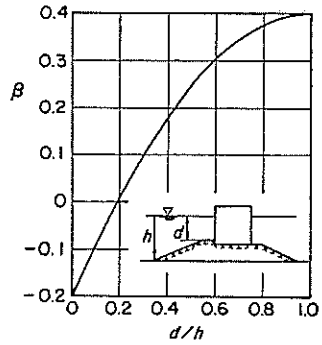

Fig. 7 Nomograph for Parameter β

where $\alpha=2.2$, and β is given in Fig. 7.

Although these are based on results by regular wave tests, the relations are applicable to the transmission coefficient of the significant wave height of irregular waves. Most breakwaters in Japan are designed with a relative crest height $h_c/H_{1/3}=0.6$, where $H_{1/3}$ is the design significant wave height mostly corresponding to a return period of 50 years. Then, the transmission coefficient is calculated by Eq. (5) as about 0.2 for the typical conditions of $d/h=0.6$ and $h'/h=0.7$.

(3) Transmission Coefficient of Mixed Type Breakwaters Covered with Wave Dissipating Concrete Blocks

The transmission coefficient of the mixed type breakwaters covered with wave dissipating concrete blocks is slightly influenced by the relative covering width to the incident wavelength in addition to the principal parameter of $h_c/H_{1/3}$.

Figure 8 shows experimental results by irregular wave tests. The significant wave heights of transmitted waves were measured at the location apart from the

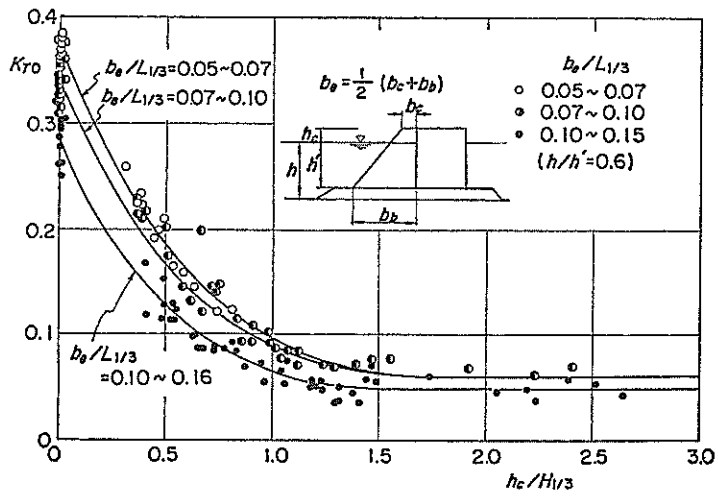

Fig. 8 Wave Transmission Coefficient for Mixed Type Breakwaters Covered with Wave Dissipating Concrete Blocks

rear face of the upright section by the distance of $(3\sim6)h$, which can be regarded as the place directly behind the breakwaters and without the direct action of overtopping water. The transmission coefficient at the location directly behind the breakwaters is denoted as K_{T0} in this paper.

The solid curves in the figure indicate the average relations of the experimental data for the different class of $b_e/L_{1/3}$, where b_e is the equivalent covering width defined by the following relation:

$$b_e=0.5(b_c+b_b). \tag{6}$$

According to the average relations, the transmission coefficients are in the range from 0.10 to 0.16 for a relative crest height of 0.6. These are smaller than the transmission coefficients predicted by Eq. (5) and demonstrate that the transmission coefficient becomes smaller when the relative covering width is wider.

(4) Change of Significant Wave Period due to Wave Transmission

So far, only the transmission coefficients directly behind the breakwaters have been presented. Some other characteristics of irregular transmitted waves, which have been obtained for mixed type breakwaters covered with wave dissipating concrete blocks, will be introduced here.

Figure 9 shows the ratio of the significant period of transmitted waves directly behind the breakwaters to that of incident waves. The data obtained by two series of experiments, made by slightly different conditions, are plotted. Although the values of the ratio of periods by both series are different, the data demonstrate that the significant wave period of transmitted waves decreases considerably from the incident significant wave period under the ordinary design condition for $K_{T0}=0.1\sim0.2$. One of the reasons why the data indicated by the square mark are smaller than the others, is that the data in the series I are analyzed by eliminating the lower frequency component from the wave profiles.[2)]

(5) Representative Wave Heights of Irregular Transmitted Waves

The distribution of wave heights of irregular transmitted waves is different from that of incident waves. Figure 10 shows an example of experimental results for the ratios of other representative wave heights to the significant wave height

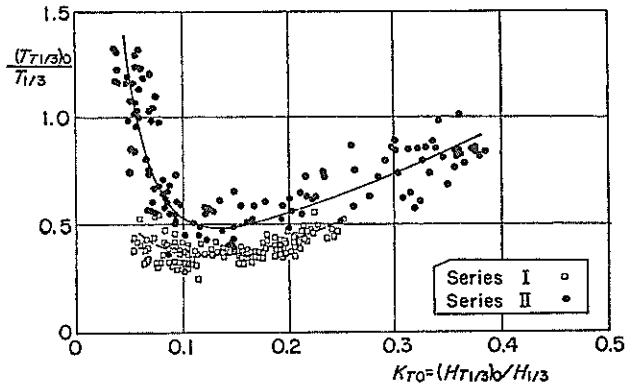

Fig. 9 Change of Significant Wave Period by Wave Transmission

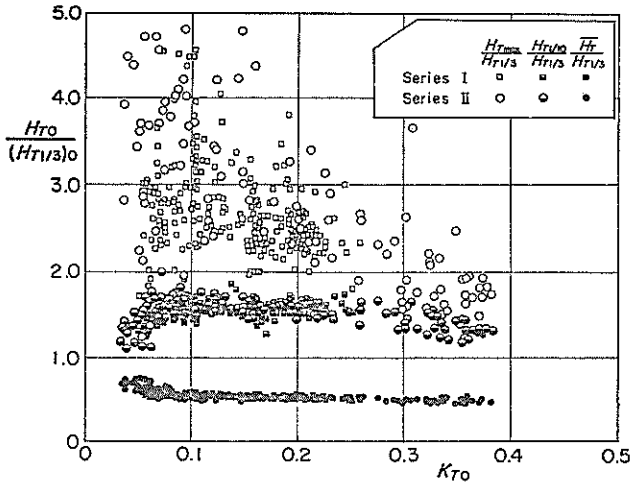

Fig. 10 Relation of Representative Wave Heights of Irregular Transmitted Waves

of transmitted waves measured directly behind the breakwaters. In particular, the ratios of the largest wave height to the significant wave height, $(H_{T\max})_0/(H_{T1/3})_0$, are greatly scattered and show a larger value than those of incident waves which are generally less than 2.0. According to these results, the following relations between the representative wave heights of transmitted waves are obtained when K_{T0} equals 0.2:

$$(H_{\max})_0/(H_{T1/3})_0 = 2.0 \sim 3.5$$
$$(H_{T1/10})_0/(H_{T1/3})_0 = 1.4 \sim 1.7$$
$$(\overline{H}_T)_0/(H_{T1/3})_0 = 0.5 \sim 0.6.$$

(6) Variation of Significant Wave Height and Period of Transmitted Waves due to Wave Propagation

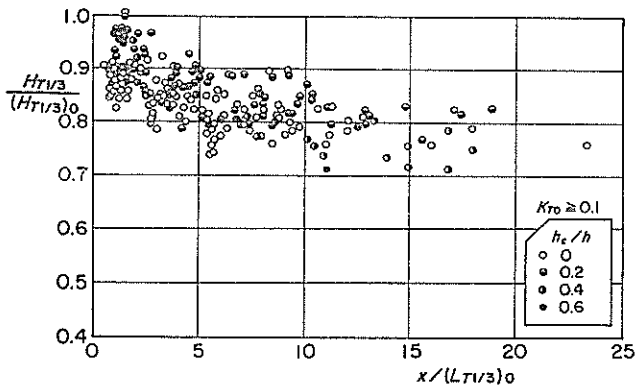

Fig. 11 Variation of Significant Wave Height of Transmitted Waves during Proprgation

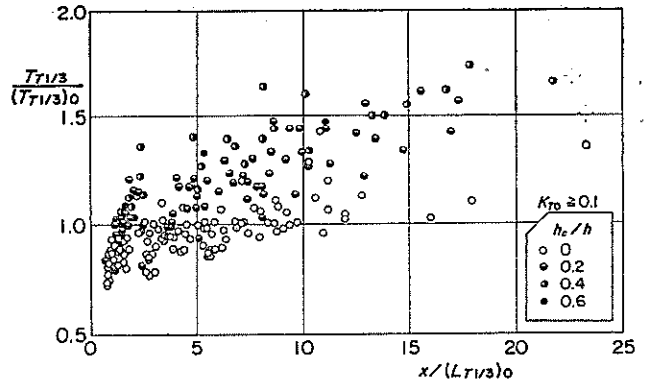

Fig. 12 Variation of Significant Wave Period of Transmitted Waves during Propagation

The irregular transmitted waves vary their properties, such as the distributions of wave height and period, when they propagate for long distances. Figures 11 and 12 show the examples of variations of significant wave height and period. In the figures, x indicates the distance from the rear face of the upright section, $(L_{T1/3})_0$ is the wavelength corresponding to the significant wave period $(T_{T1/3})_0$ directly behind the breakwater, and $H_{T1/3}$ and $T_{T1/3}$ are the significant wave height and period at the location of arbitrary distance, respectively. The tendency is noticed that the significant wave height decreases and the significant wave period increases as the transmitted waves propagate for a long distance, although the data are considerably scattered.

2.4 Wave Forces on the Upright Section

(1) Generalized Goda Formula

Wave forces on the upright section are the most important environmental force in the design of mixed type breakwaters. Therefore, much effort has been made to study the wave forces on the upright section. As a result of those studies, a formula to calculate the design wave forces has been established by Goda (1973).[3] This formula is being successfully applied to the design of mixed type breakwaters in

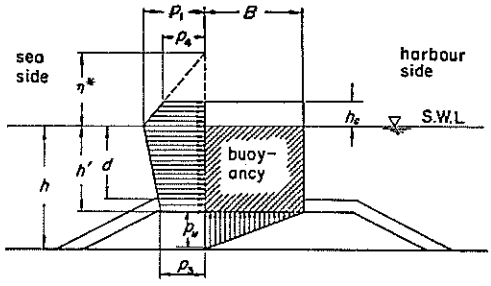

Fig. 13 Distribution of Design Wave Pressure

Japan. The Goda formula, by which the wave pressure distribution is given as shown in Fig. 13, can be written in a generalized form as follows:

$$\eta^*=0.75(1+\cos\beta)\lambda_1 H_D \tag{7}$$

$$p_1=0.5(1+\cos\beta)(\alpha_1+\lambda_2\alpha_2\cos^2\beta)w_0\lambda_1 H_D \tag{8}$$

$$p_3=\alpha_3 p_1 \tag{9}$$

$$p_4=\alpha_4 p_1 \tag{10}$$

$$p_u=0.5(1+\cos\beta)\lambda_3\alpha_1\alpha_3 w_0 H_D \tag{11}$$

$$\alpha_1=0.6+\frac{1}{2}\left[\frac{4\pi h/L_D}{\sinh(4\pi h/L_D)}\right]^2 \tag{12}$$

$$\alpha_2=\min\left\{\frac{h_b-d}{3h_b}\left(\frac{H_D}{d}\right)^2,\ \frac{2d}{H_D}\right\} \tag{13}$$

$$\alpha_3=1-\frac{h'}{h}\left[1-\frac{1}{\cosh(2\pi h/L_D)}\right] \tag{14}$$

$$\alpha_4=1-\frac{h_c^*}{\eta^*} \tag{15}$$

$$h_c^*=\min\{\eta^*,\ h_c\} \tag{16}$$

where,

η^* : hypothetical extreme height of pressure above the still water level
p_1 : pressure intensity at the still water level
p_3 : pressure intensity at the bottom level of the upright section
p_4 : pressure intensity at the crest level of the upright section
p_u : toe pressure on the bottom of the upright section
w_0 : specific weight of sea water
h_b : water depth at the location offshore side by the distance of five times of significant wave height from the wall
H_D : wave height used in the calculation of design wave forces
L_D : wavelength used in the calculation of design wave forces
β : angle of wave approach to the breakwater (see Fig. 14)

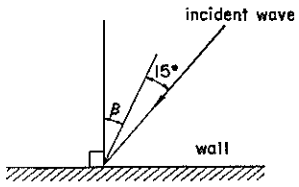

Fig. 14 Angle of Wave Incidence

$\min(a, b)$: smaller value of a or b
$\lambda_1, \lambda_2, \lambda_3$: modification factors of wave pressure depending on the structure type.

In the design calculations, the largest wave height of the design waves and the wavelength corresponding to the design significant wave period are applied to H_D and L_D.

(2) Wave Forces on the Upright Section of Mixed Type Breakwaters

For the upright section of mixed type breakwaters as well as vertical break-

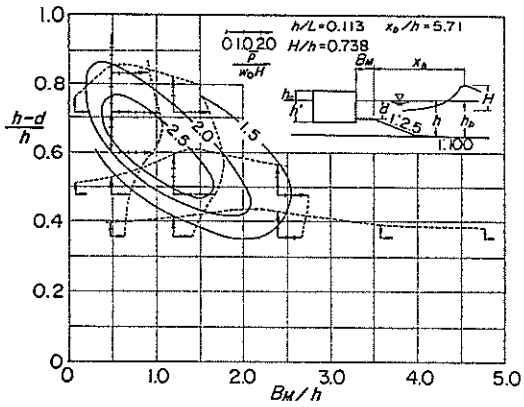

Fig. 15 Example of Wave Force Variation due to Mound Configulation

waters, the modification factors of $\lambda_1=\lambda_2=\lambda_3=1.0$ are applied since the Goda formula has been proposed originally to this type of breakwaters.

Although the Goda formula can be successfully applied to the design of the upright section in most cases, it fails to predict the wave forces under limited conditions. One of them is the wave forces on the upright sections with large and high rubble mound foundations[4]. For example, Fig. 15 demonstrates the variation of the wave pressure intensity $\bar{p}$ averaged over the total height of the upright section. In the figure, the abscissa indicates the relative berm width of the rubble mound foundation to the water depth, and the ordinate indicates the relative thickness of the rubble mound foundation including the armour layer to the water depth. The data are obtained on the basis of sliding test of the upright sections for different sizes of the rubble mound foundations. Therefore, the wave pressure intensity can be considered as an intensity equivalent to the sliding.

In the figure, the variation of the intensity is shown by the lines of constant values of $\bar{p}/w_0H$ for a wave condition of $h/L=0.113$ and $H/h=0.738$. This example shows the fact that the wave pressure intensity is greatly influenced not only by the height of the rubble mound foundation but also by the berm width, and that the breaking wave pressures become very large when the rubble mound foundation is unfavourably high and wide. Since the influence of the berm width is not considered in the Goda formula and the predicted non-dimensional intensity by the Goda formula is 2.0 at most, there must be no doubt that the Goda formula is not perfect and fails to predict the wave forces in the limited conditions. In spite of this fact, the Goda formula is very useful as a design wave force formula, because such a breakwater section receiving extraordinarily large wave pressures should not be adopted from the viewpoint of the stability and the construction cost. In fact, the low rubble mound foundation $d/h>0.6$ is strongly recommended when breaking waves act on breakwaters perpendicularly.

(3) Wave Forces on the Upright Section Covered with Wave Dissipating Concrete Blocks

Wave forces on the upright section are reduced by covering with wave dissipating concrete blocks. In particular, no strong impulsive pressures by breaking

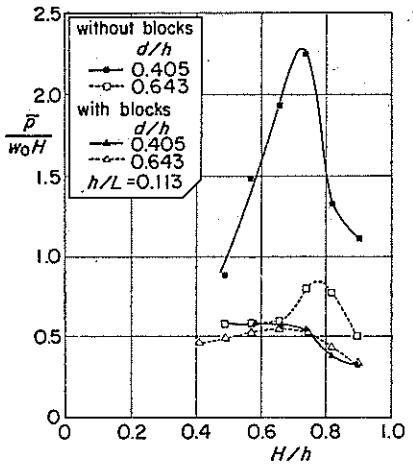

Fig. 16 Change of Impulsive Wave Pressure by Covering with Wave Dissipating Concrete Blocks

waves act on the upright section covered sufficiently. Figure 16 demonstrates how the pressure intensities averaged over the total height of the upright section are different with and without wave dissipating concrete blocks. It is noticed that the intensity is decreased greatly in the case of a high rubble mound foundation of $d/h=0.405$ for which impulsive pressures act on the upright section without the covering.

The wave forces on the upright section covered with wave dissipating concrete blocks can be calculated by the generalized Goda formula and using the following modification factors[5]:

$$\lambda_1=\lambda_3=0.8\sim1.0 \text{ and } \lambda_2=0.$$

The range of the factors λ_1 and λ_3 may correspond to the difference of the relative covering width to the wavelength, but it is not formulated. When the upright section is sufficiently covered with wave dissipating concrete blocks, the lower value of 0.8 is commonly applied. It should be kept in mind that the wave forces are greatly increased in many case if the covering is not sufficient as in a breakwater at the stage under construction.

2.5 Stability of Armour Units for the Rubble Mound Foundation

(1) Stability Equation

For mixed type breakwaters, not only the upright section but also the rubble mound foundation must be stable against the wave action. In order to maintain stability, an armour layer with large size stones or concrete blocks is placed for the rubble mound foundation. The following stability equation, which was derived by Hudson (1959)[6], is frequently applied to calculate the stable weight of armour units.

$$W=\frac{\gamma_r}{N_s^3(S_r-1)^3}H^3 \tag{17}$$

where,

W : weight of individual armour unit

γ_r : specific weight of armour unit

S_r : specific gravity of armour unit, relative to the water

H : wave height applied to the calculation, usually the significant wave height

N_s : stability number of armour unit.

The stability number N_s in Eq. (17) depends on such variables as shape of armour unit, manner of placing, shape of rubble mound foundation, wave conditions (wave height, period, duration) and so on. It must be appropriately determined taking into consideration these influential factors on the basis of adequate test results.

(2) Stability Number for Quarry Stones

Tanimoto et al. (1982)[7),8)] have proposed the following formula to calculate the stability number for quarry stones on the basis of analytical considerations and irregular wave tests:

$$N_s=\max\{1.8,\ 1.3\alpha+1.8\exp[-1.5\alpha(1-\kappa)]\} \tag{18}$$

$$\alpha=\{(1-\kappa)/\kappa^{1/3}\}(h'/H_{1/3}) \tag{19}$$

$$\kappa=\kappa_1\kappa_2 \tag{20}$$

$$\kappa_1=(4\pi h'/L')/\sinh(4\pi h'/L') \tag{21}$$

$$\kappa_2=\sin^2(2\pi B_M/L') \tag{22}$$

where,

L' : wavelength corresponding to the significant wave period at the depth h'.

In these formulations, the stability number is the function of three major parameters of $h'/H_{1/3}$, h'/L', and B_M/L'.

(3) Relation between Weight and Damage Percent

Figure 17 shows the damage percent D obtained by the laboratory experiments,

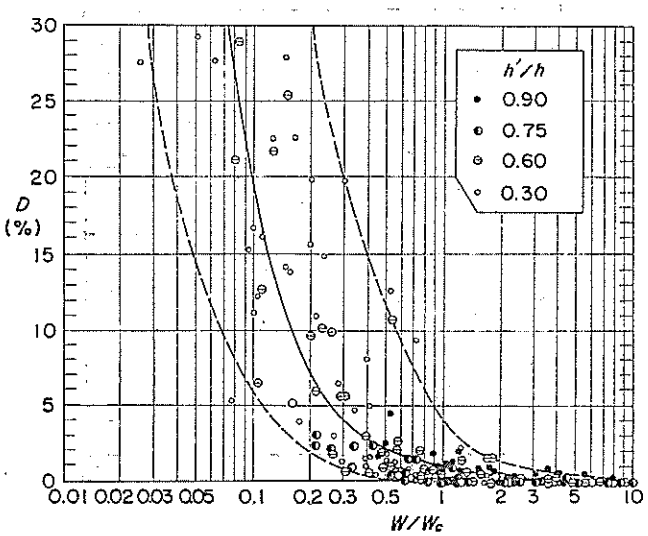

Fig. 17 Experimental Results of Damage Percent

where W is the mean weight used in the experiments and W_0 is the weight calculated by Eqs. (17) through (22). The data are considerably scattered and the value of W/W_0 for $D=5$, for example, extends from 0.1 to 1.0. This comes from the essential properties for the stability of rubble structures as well as inaccuracies in the formulation of the stability number. Another example of the variability in the stability of rubble structures will be discussed later. The test results in Fig. 17 indicate that the proposed method to evaluate the stability number is slightly on the safe side and the damage percent of the armour stones with the calculated weight is less than 5.

2.6 Stability of Wave Dissipating Concrete Blocks

(1) Hudson's Formula

Hudson's formula is commonly applied to investigate the stable weight of armour units for the sloping structures. The stability of wave dissipating concrete blocks for the mixed type breakwaters is also investigated by Hudson's formula as:

$$W=\frac{\gamma_r}{K_D(S_r-1)^3\cot\alpha}H^3 \tag{23}$$

where,

α : angle of structure slope measured from the horizontal plane

K_D : stability coefficient of armor unit.

The stability coefficient K_D in Eq. (23) must be the function of various parameters related with structural and hydraulic conditions, but it is not formulated well, in spite of the fact that a great number of studies have been carried out in the world. One of the reasons may be the variability in the stability.

(2) Variability in the Stability

Figure 18 shows the experimentally derived relations for the damage percent

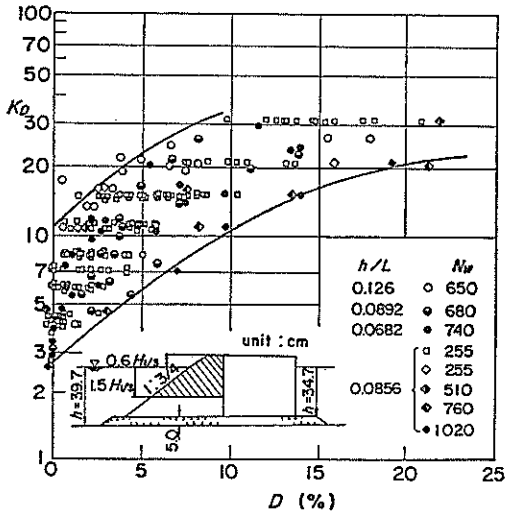

Fig. 18 Experimental Relation Between Damage Percent and K_D Value

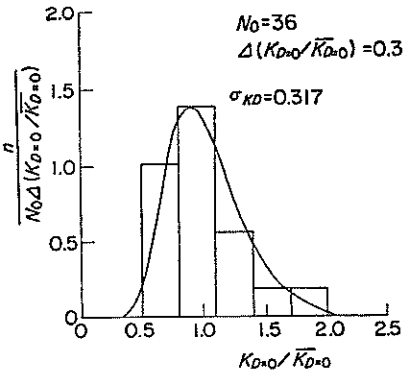

Fig. 19 Distribution of K_D Value

and the K_D-value for various irregular wave conditions, for the same shape of concrete blocks. The experiments were carried out in the same wave channel, by the same procedures, and by the same criteria of damage[9]. Nevertheless, the results are greatly scattered and it is not possible to determine only one value of K_D. There may be two reasons for these variations. The one is the difference of wave conditions (relative wave height, relative water depth, and the duration of different wave trains) and the other is the variability in the stability. Here, only the latter will be referred to.

The results presented in Fig. 18 include data obtained repeatedly by the same conditions for the significant wave period and the duration. Figure 19 shows the normalized distribution of the K_D value corresponding to the critical state of $D=0$ for the repeated experimental results. According to the results, the coefficient of variance is 0.32 and the variation due to the repeated tests is not different from the variation due to the difference of wave conditions in these experiments. This implies that the stability of the rubble structures must be investigated by a sufficient number of data.

Based on the results by repeated tests, Tanimoto et al. (1985)[9] have derived the following relation to estimate the standard deviation of the damage percent at the arbitrary level:

$$\sigma_D/\overline{D}=0.89\overline{D}^{-0.57} \tag{24}$$

where $\overline{D}$ and σ_D are the expected value and the standard deviation of the damage percent.

3. Breakwater Structures Utilizing Wave Forces

3.1 Basic Shapes of Wave Barrier Wall

The principal function of breakwaters is to stop the wave propagation there, and the simplest method is to intercept the water by a solid wall. This solid wall is called a wave barrier wall in this paper. The shape of this wave barrier wall can be considered arbitrary, but the basic four shapes as shown in Fig. 20 are

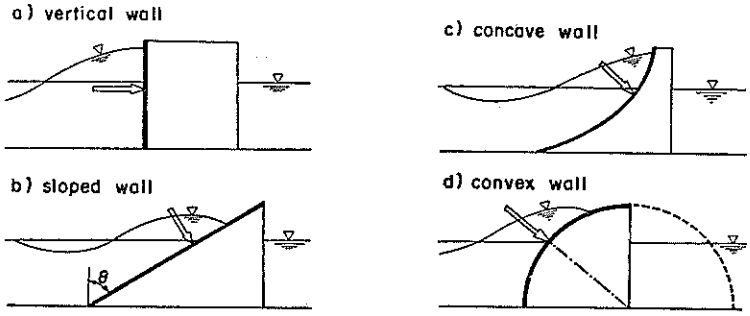

Fig. 20 Basic Shapes of Wave Barrier Wall

discussed for their fundamental characteristics and their applications to breakwater structures.

a) Vertical wall

The length of wall to intercept the water is the shortest. However, the weight, the width in other words, sufficient to resist the wave forces is necessary in the case of gravity type structures. The wave reflection from the wall is high and the horizontal wave pressure acts on the wall almost with the same phase, as described before.

b) Sloped wall

Since the sloped wall is an inclined vertical wall, the length of wall to intercept the water becomes longer. One remarkable feature of this wall is that the wave pressure has a downward component because it acts perpendicularly to the wall face. Consequently, the stability of gravity type structures with sloped walls against wave forces is improved. It has the disadvantage, however, that waves may pass over its top more easily and generate transmitted waves when the crest height is limited.

c) Concave wall

Concave walls have similar characteristics to those of sloped walls. Although the length of the wall becomes shorter than that for sloped walls, the direction of the resultant wave force on the wall shifts towards the horizontal.

d) Convex wall

Convex walls also have similar characteristics to sloped walls. The distinguished feature of this wall appears when the section is a semi-circle. In this case, the resultant wave force acts on the center of the circle and gives no rotational force.

Among the wave barrier walls mentioned above, vertical walls are commonly applied to breakwaters as vertical breakwaters and the upright section of the mixed type breakwaters for which the hydraulic aspects are already described previously in Chapter 2. Therefore, the applications of the other wave barrier walls to breakwaters are considered furthermore in this Chapter.

3.2 Sloped Wall Breakwaters

(1) Sloped Caisson

A wave force having a downward component acts on the wall with a sloped, concave, and convex face at the phase of the wave crest. Because the downward component works as a weight to resist sliding, breakwaters having these wave barrier walls can be said to be breakwaters utilizing the wave forces to resist wave

forces.

A typical structure is a caisson with a sloped face. Consider an ideal structure with a sloped face as shown in the second figure of Fig. 20, and denote the angle of the slope to the vertical as θ, and the resultant wave force acting on the wall as F_S. Then, the horizontal and vertical components of F_S are expressed as

$$F_H=F_S\cos\theta,\quad F_V=F_S\sin\theta \tag{25}$$

Now, select the angle θ so that the horizontal component of the wave force is equivalent to the frictional force due to the vertical component, and denote the angle as θ_0. Namely,

$$F_H=\mu F_V,\quad \cot\theta_0=\mu \tag{26}$$

where μ is the friction factor between the bottom of structure and the foundation. When the value of μ is 0.6 which is a standard value for the concrete slab and the rubble mound foundation of quarry stones, the value of θ_0 is about 60 degrees. This implies that a caisson having a slope of $\theta=60°$ is always stable against sliding due to the action of waves, if it has only the weight resisting against the uplift force acting underneath the bottom slab.

(2) Sloping Top Caisson

It is difficult, however, to make a sloped face for the whole height of the structure. Therefore, the actual applications are more feasible to make a sloped face only at the upper part of the front wall. This structure is called as the sloping top caisson as shown in Fig. 21.

Morihira and Kunita (1979)[10] have proposed the modification method of Goda's formula to calculate the design wave forces as explained in Fig. 22. According to the method, the force F_S, which is acting on the sloped face perpendicularly, is expressed as

$$F_S=P_S\cos\theta \tag{27}$$

where P_S is the force integrated in the wave pressure distribution by the Goda formula for the range of the corresponding height h_S to the sloped face.

In general, the wave transmission over the sloping top caisson is larger than that over the ordinary vertical caisson when the crest heights are the same. The sloping top caisson having a crest height of $h_c=1.0\,H_{1/3}$ is generally recommended for the conditions of $\theta=45°$ and $h_S=h_c$, then the wave transmission can be considered as the same to that of the ordinary vertical caisson having a crest height of $h_c=0.6\,H_{1/3}$. Based on the proposed design method, such sloping top caisson breakwaters

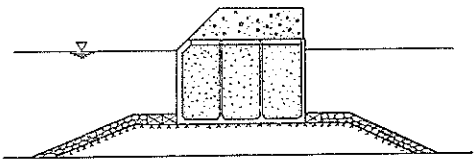

Fig. 21 Sloping Top Caisson

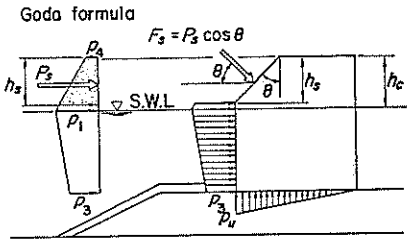

Fig. 22 Wave Force on Sloping Top Caisson

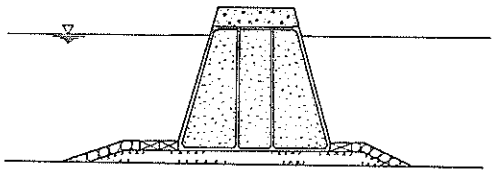

Fig. 23 Trapezoidal Caisson

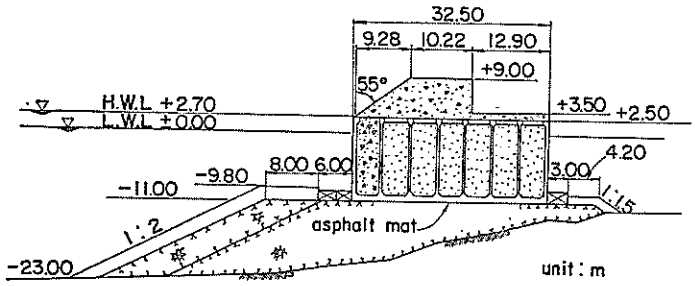

Fig. 24 Cross Section of Sloping Top Caisson Breakwater at Katadomari Port

of $\theta=45°$ have been already constructed in several ports (Niigata, Sakata, Miyazaki) in Japan.

(3) Trapezoidal Caisson

Another feasible application of the sloping wall is the trapezoidal caisson shown in Fig. 23. The hydraulic characteristics of this caisson had been investigated by laboratory experiments and the method for calculating the design wave forces has been proposed[11].

(4) Sloping Top Caisson Breakwater under Construction at Katadomari Port

As to the trapezoidal caisson, further discussion will be given later in Chapter 4. Here, an example of the sloping top caisson breakwaters is introduced.

Katadomari Port is located at a small island called Kuroshima in the southwest of Japan. A breakwater with a length of 120 m, of which the lee side serves for berthing, had been constructed by the summer of 1987. The breakwater was severely damaged by high waves at the occasion of Typhoon 8712 in the end of August. After the damage, it has been decided that the breakwater is to be reconstructed with sloping top caissons. Figure 24 shows the cross section at the head of the extension. The section is designed to the wave condition of $T_{1/3}=12.6$ s, $H_{1/3}=9.5$ m, and $H_{max}=17.1$ m.

3.3 Concave Wall Breakwaters

(1) Multi-cellular Caisson

Although the concave wall is being frequently applied to sea walls, there is no example of application to breakwaters. Goullet[12] proposed the breakwater of concave cyclopian block, but this has not been realized.

Tanimoto et al. (1981)[13] have studied the multi-cellular caisson as shown in

Fig. 25. This caisson consists of triple-layered slopes with the rear end bended upwardly. The spaces formed between these slopes are opened at the both ends of the vertical front and the horizontal top of caisson. The idea of the multi-cellular caisson is explained in Fig. 26. The idea starts from the sloped wall. The concave wall is then conceived to reduce the width. Finally, the concave wall is divided into three segments and piled up vertically to become a compact structure. The hydraulic experiments establish that a multi-cellular caisson having a relatively narrow width is very stable against wave forces and that the reflected waves are greatly reduced when the vertical slit wall is attached at the front as shown in Fig. 27.

(2) Wave Reflection and Transmission

Figure 28 shows the reflection and the transmission coefficients of the multi-cellular caissons with and without the vertical slit wall. Two definitions of the crest height, h_{c1} and h_{c2}, are explained in the figure. According to these test results, the crest heights corresponding to $K_T=0.2$ are as follows:

Caisson of $h_{c2}=0.5h_{c1}$ without slit wall; $h_{c1}=(1.0\sim1.1)H_{1/3}$

Caisson of $h_{c2}=h_{c1}$ without slit wall; $h_{c1}=(0.8\sim0.9)H_{1/3}$

Caisson of $h_{c2}=0.5h_{c1}$ with slit wall; $h_{c1}\fallingdotseq0.75H_{1/3}$.

The reflection coefficient of the caisson with the slit wall is in the range from 0.4 to 0.5 for the waves of $h/L_{1/3}=0.092$. However, it varies with the wave conditions, and especially with the wave period. For the most favourable wave conditions, the reflection coefficient is reduced to 0.2.

The hydraulic characteristics of caissons with vertical slit walls vary with the opening ratio ε defined as

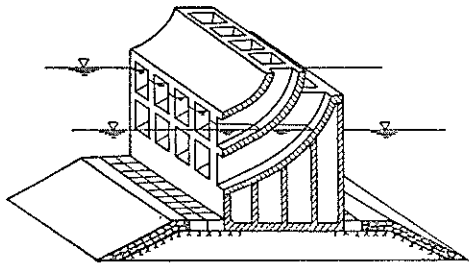

Fig. 25 Multi-cellular Caisson

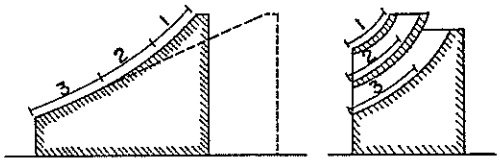

Fig. 26 Idea of Multi-cellular Caisson

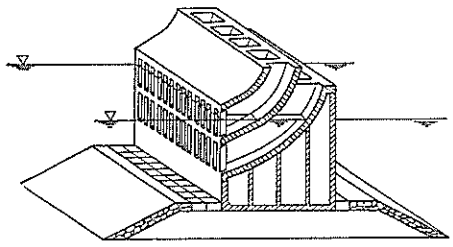

Fig. 27 Multi-cellular Caisson with Slit Wall

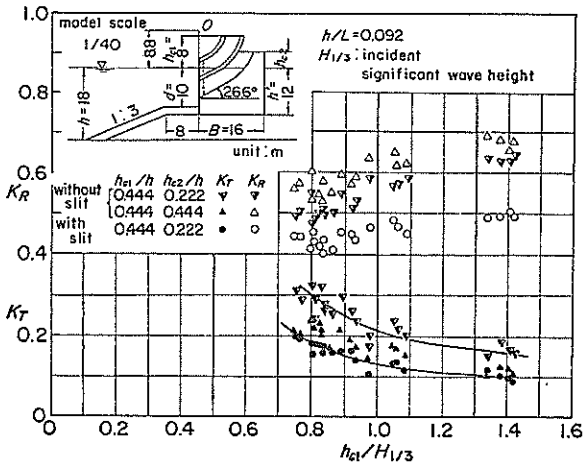

Fig. 28 Reflection and Transmission Coefficients of Multi-cellular Caisson

$$\varepsilon = s/(D+s) \tag{28}$$

where, D is the width of the slit member, and s is the width of the gap. The opening ratio of the slit wall tested in this study is 1/3.

(3) Wave forces

The design wave forces to examine the stability of the caisson can be calculated for a hypothetical distribution of wave pressure as shown in Fig. 29, where the caisson is replaced by a vertical solid wall with the same height and the horizontal wave force on the caisson is calculated by the hypothetical wave pressures on the replaced solid wall. The pressure intensities are calculated by the generalized Goda formula with the following modification factors:

Caisson without the slit wall; $\lambda_1=0.6$, $\lambda_2=0$

Caisson with the slit wall; $\lambda_1=0.8$, $\lambda_2=0$.

In this method, the vertical component of wave forces is disregarded on the assumption that the downward component of the wave forces on the triple-layered slopes and the uplift force underneath the bottom slab cancel each other out.

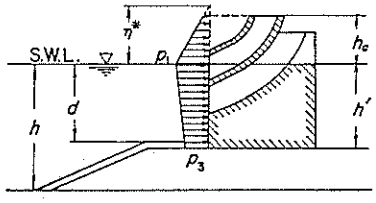

Fig. 29 Wave Pressure Distribution of Multi-cellular Caisson for the Stability Design

The wave forces on each member must be given for the design of structural strength. For this purpose, the following intensities, which are supposed to act uniformly on each member, are proposed:

Uppermost bending slope; $f=0.75w_0H, (-0.5w_0H)$
Secondary bending slope; $f=0.5w_0H, (-0.5w_0H)$
Bottom bending slope; $f=0.75w_0H$
Side wall in the hollow; $f=0.5w_0H, (-0.5w_0H)$
Vertical slit member; $f=0.75w_0H, (-0.5w_0H)$.

where, the negative intensities in ( ) indicate those with the opposing direction towards the seaside excepting the side wall in the hollow. The positive and the negative intensities must be separately considered, because they correspond to the different phases. The negative intensity for the bottom bending slope can be obtained as the change of static water pressure when the water level is lowered by $0.5H$ from the still water.

(4) Field Test of Multi-cellular Caisson at Wakayama Port

A full size unit of the multi-cellular caisson was fabricated in 1985, and is being tested in the actual sea at Wakayama Port. Figure 30 shows the cross section of the test caisson, which is designed for the wave conditions of $T_{1/3}=12.0$ s, $H_{1/3}=5.0$ m, and $H_{max}=9.0$ m. Photo 2 shows the front view of the test caisson, which is installed between the ordinary caisson breakwaters.

3.4 Convex Wall Breakwaters

The author has proposed the curved slit caisson having a convex slit wall. However, the structure of this caisson is shown later, because the idea is related to the wave dissipating caisson.

The distinguished merit of convex wall appears when the section is a semi-circle as shown in Fig. 31. As mentioned before, the wave pressures on the semi-circle face act towards the center. Consequently, the resultant force acts towards the center and makes no rotational moment. It results in a quasi-uniform distribution of the reaction at the bottom slab, although the uplift force having a triangular distribution acts at the bottom. This merit may be used as a breakwater on the

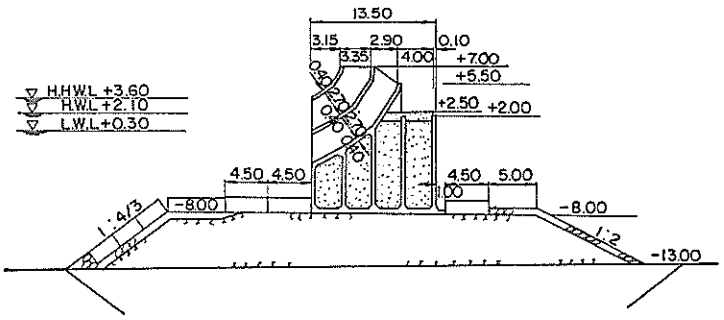

Fig. 30 Cross Section of Multi-celluar Caisson Breakwater at Wakayama Port

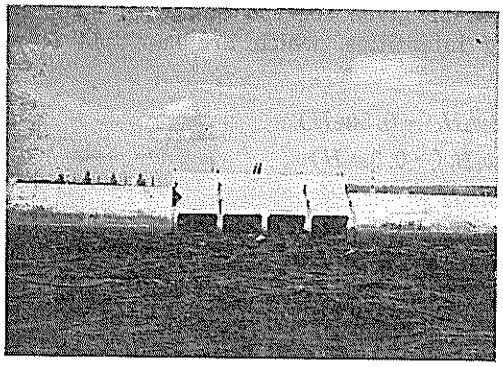

Photo 2 Multi-cellular Caisson

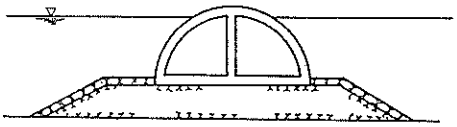

Fig. 31 Breakwater with Semi-circular Section

very soft ground. The hydraulic characteristics such as wave reflection, transmission, and forces of semi-circular section breakwaters have been investigated by laboratory experiments[14].

4. Breakwater Strucures Absorbing Waves

4.1 Vertical Partially-hollow Wall and Wave Dissipating Caisson Breakwaters

The wave barrier walls discussed in Chapter 3 are the walls by which the water is perfectly intercepted. There are other types of breakwaters that allow some energy to pass through them. Curtain breakwaters having the impermeable vertical wall only near the water surface are typical ones, and they have been constructed in many ports. A steel pile breakwater having small gaps is another example of such breakwaters. In the case of breakwaters with some openings, part of incident wave energy is dissipated but another part is transmitted behind them generating waves which propagate towards the shore. Such structures, however, have limitation that their application to rough sea conditions is not practical from the standpoint of the structural strength as well as the performance of wave dissipation. Therefore, an impermeable structure having a partially-hollow wall and a wave chamber is considered so that the mechanism of wave dissipation is kept and waves are stopped there as a whole. Such a structure is proposed by Jarlan (1961)[15] at first as the perforated caisson and is generally called the wave dissipating caisson in this paper.

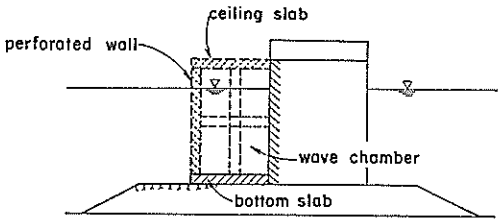

Fig. 32 Structural Elements of Wave Dissipating Caisson

Figure 32 shows a schematic diagram of structural elements of the wave dissipating caisson. The wave dissipating caisson consists of a perforated front wall and a wave chamber, and various variations are considered by the combination of different structural elements. In general, the wave dissipating caisson has the following merits:

a) Wave reflection is decreased.
b) Wave transmission due to overtopping is decreased.
c) Wave force is decreased.

4.2 Curved Slit Caisson Breakwaters

(1) Shape of the Structure

The curved slit caisson as shown in Fig. 33 is one kind of wave dissipating caisson. The perforated front wall of the caisson is an arc-shaped wall, and the shape of wave chamber with a horizontal bottom and a vertical rear wall is a quarter circle in side view. The idea of the curved slit caisson is explained in Fig. 34. It was originally a combination of a sloping wall caisson and an ordinary wave dissipating caisson, and then the slit wall is shaped up to a circular arc because of the structural reasons. From 1976 to 1983 intensive investigations had been carried out to study the hydraulic characteristics and to establish the design and execution methods in the laboratory[16] and in the field.

(2) Wave Reflection and Transmission

The hydraulic characteristics of the curved slit caisson vary with the opening ratio of the slit wall. Based on the test results for wave reflection for various

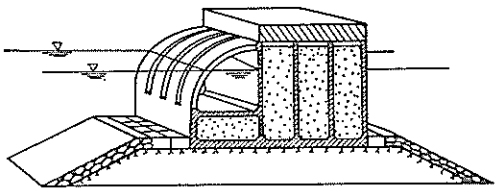

Fig. 33 Curved Slit Caisson

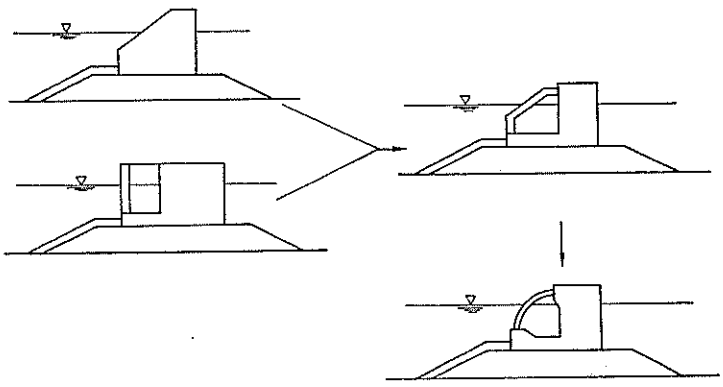

Fig. 34 Idea of Curved Slit Caisson

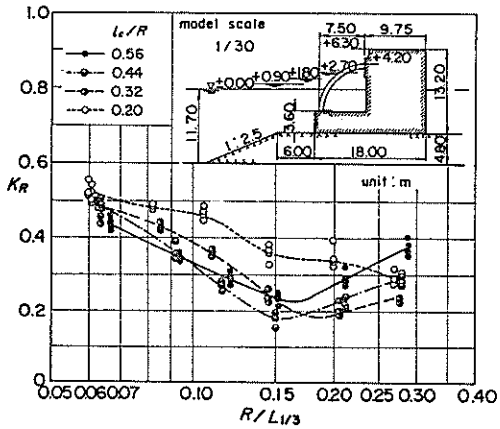

Fig. 35 Reflection Coefficient of Curved Slit Caisson

opening ratios, the optimum value was selected to be 0.25 for the definition by Eq. (28).

Figure 35 shows the reflection coefficient of the caisson with $\varepsilon=0.25$, where R is the outer radius of the curved slit wall, and l_c is the top height of the curved slit wall above the still water level. Because the curved slit wall is submerged when the top is too low, the reflection coefficient of the caisson with $l_c/R=0.20$ is higher than that of others. In general, a top height larger than $l_c/R=0.3$ is recommended. Then the wave absorbing capacity of the curved slit caisson breakwaters can be considered to be almost the same as that of the mixed type breakwaters covered with wave dissipating concrete blocks.

As for the wave transmission, the transmission coefficient of the curved slit caisson is slightly less than that of an ordinary caisson without a wave chamber. Therefore, the crest height of the upright section can be favourably determined as the same height as ordinary caisson breakwaters.

(3) Wave Forces

A remarkable feature of the wave forces on the curved slit caisson is the appearance of impulsive pressures inside the wave chamber, at the instance when the wave chamber is completely covered by the water. Considering this feature, the wave pressure distributions, which are applied to the design of structural strength, have been proposed as shown in Fig. 36. The phase 1 corresponds to the time

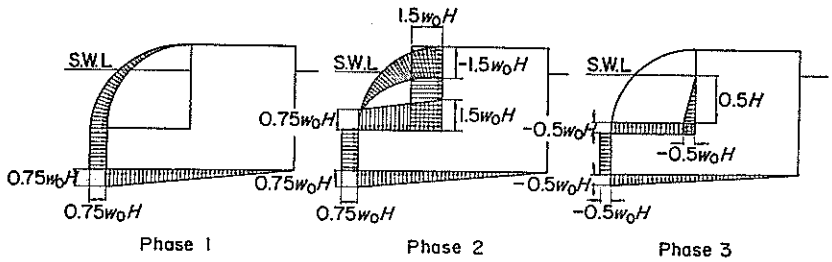

Fig. 36 Wave Pressure Distribution for the Design of Strength

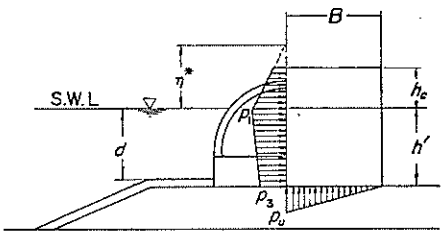

Fig. 37 Wave Pressure Distribution for the Stability Design

directly before when the wave chamber is covered by the water, the phase 2 corresponds to the instance when the wave chamber is completely covered by the water, and the phase 3 corresponds to the phase at the wave trough. The force intensity f perpendicularly on the curved slit member at an arbitrary location is expressed as

$$f=f_A \cos^2\theta+f_B \sin^2\theta \tag{29}$$

where θ is the angle between the application line and the horizontal plane, and

$f_A=0.75w_0H$, $f_B=0$; at the phase 1

$f_A=0$, $f_B=-1.5w_0H$; at the phase 2.

The wave forces applied to examine the stability of the caisson can be easily calculated by the generalized Goda formula for the hypothetical upright section disregarding the wave dissipating section of curved slit wall as shown in Fig. 37. The modification factors in this case are as follows:

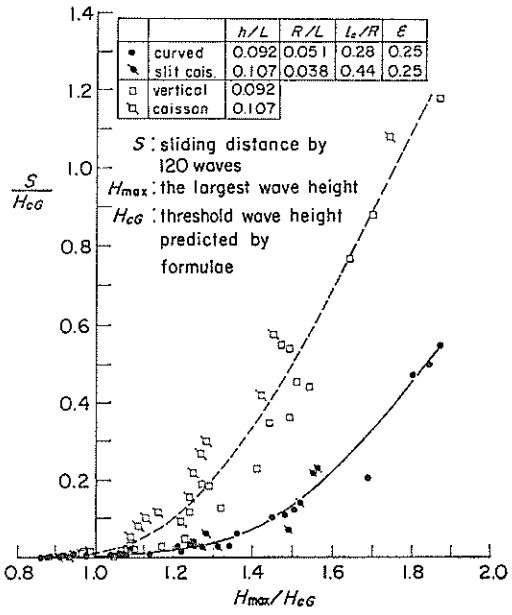

Fig. 38 Experimental Results of Sliding

$\lambda_1=\lambda_3=1.0,\ \lambda_2=0.$

Figure 38 shows the results of sliding tests in the laboratory for both breakwaters of the ordinary caisson and the curved slit caisson, where S is the sliding distance by the action of about 120 irregular waves, H_{max} is the largest wave height of each wave trains, and H_{cg} is the critical wave height calculated by the Goda formula for the ordinary caisson and by the proposed method for the curved slit caisson. The results demonstrate that the curved slit caisson breakwater designed by the proposed method is safer than an ordinary caisson breakwater designed by the Goda formula, because the sliding distance of the former remains less than the latter even if the wave height exceeds the design value.

(4) Curved Slit Caisson Breakwater at Funakawa Port

A curved slit caisson breakwater of 150 m in the length was completed in the construction at Funakawa Port in 1984 by the First District Port Construction Bureau. Figure 39 shows the standard cross section. The design wave conditions are $T_{1/3}=8.7$ s, $H_{1/3}=5.5$ m, and $H_{max}=9.9$ m. The curved slit members are prefabricated with the prestressed concrete and fixed to the caisson by the dry joint method. Photo 3 shows the curved slit caissons being placed temporarily at Akita Port. Although the breakwaters have been attacked by severe waves of the design magnitude several times after the completion, they remain intact without showing any behaviour

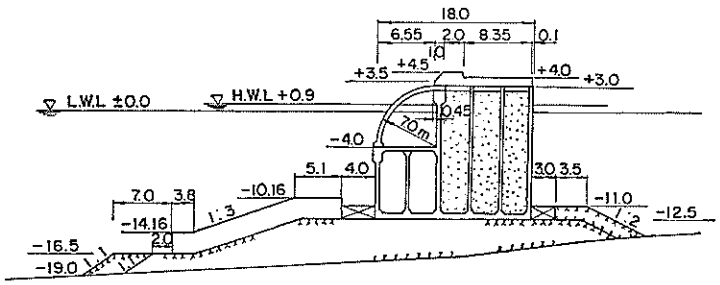

Fig. 39 Cross Section of Curved Slit Caisson Breakwater at Funakawa Port

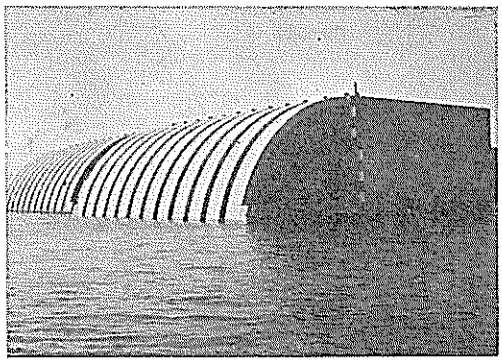

Photo 3 Curved Slit Caissons Placed Temporarily

beyond predictions by previous studies.

4.3 Wave Power Extracting Caisson Breakwaters

(1) Shape of the Structure

Although the wave energy is just dissipated by the wave dissipating caisson breakwaters, the wave energy can be converted into usable energy by a specially-devised caisson breakwater illustrated in Fig. 40. The caisson is called the wave power extracting caisson and has an air chamber attached to the front of the ordinary concrete caisson. Waves enter into the air chamber through an opening under the curtain wall, and cause the vertical oscillation of the water surface in the air chamber. Then, air in the upper half of the air chamber is compressed when the water surface rises, and is expanded when the water surface falls. The air motion generates a high-velocity flow through the nozzle which activates an air turbine to generate electricity, if an air turbine and an electric generator are installed in the caisson. A combination of the wave power converter and the caisson breakwater is attractive because the construction cost can be jointly borned by the accounts for power generation and harbour protection.

Since the wave power extracting caisson is one of the wave dissipating caissons, it is expected to have similar advantageous characteristics. The wave power extracting caisson has an inclined upper front wall. It therefore has the same characteristics as the sloping top caisson in Chapter 3.

The study on the wave power extracting caisson breakwater was started in 1982 as a 5-year special project. Six reports were already published on the study, but they mainly described on the aspects as the wave power converter[17)~22)]. The thermodynamics and wave-kinematics method which predicts the conversion from wave power to electric power was established and the design method of the converter including the turbine and generator was proposed in the reports. In this section, the wave power extracting caisson breakwater is briefly discussed with respect to its function and stability as a breakwater, based on the experimental results recently conducted.

(2) Wave Power Conversion Efficiency, Reflection Coefficient and Transmission Coefficient

The conversion efficiency from wave power to air power in the air chamber is

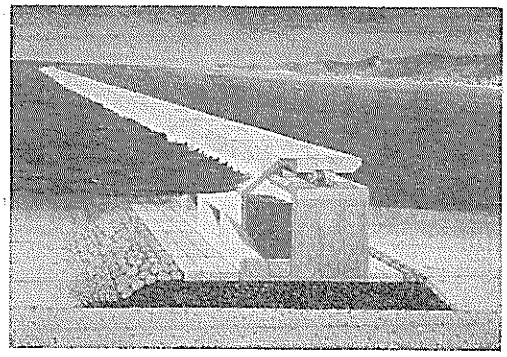

Fig. 40 Wave Power Extracting Caisson Breakwater

the most important factor not only as a wave power converter but also as a breakwater because the higher conversion efficiency yields the lower reflection coefficient. The conversion efficiency is relatively large when the air chamber width B_a ranges from 0.1 to 0.2 $L_{1/3}$, and the chamber width B_a is usually recommended to be 0.13 $L_{1/3}$. The conversion efficiency also depends on the relative water depth $h/L_{1/3}$ and the opening ratio ε of the air nozzle. When the relative water depth is small and the opening ratio is about 1/200, the conversion efficiency is more than 0.7.

Figure 41 shows the reflection coefficient of the wave power extracting caisson breakwater (WPEC). The reflection coefficients of a sloping top caisson (STC) and a sloping top caisson covered with wave dissipating concrete blocks (STC-B) are also shown in the figure. The width B of the model wave power extracting caisson in the experiments was 135 cm, the bottom depth h' was 72.5 cm, the crest height h_c was 55 cm, the air chamber width B_a was 35 cm and the water depth h was 97.5 cm. The model of the sloping top caisson was almost the same as the model of the wave power extracting caisson, but did not have the opening in the front wall. The reflection coefficient of the wave power extracting caisson is about 0.45 when the wave height is relatively small. The reflection coefficient is about 0.55 even when the wave height is large. The reflection coefficient of the wave power extracting caisson is much smaller than the sloping top caisson, but larger than that of the sloping top caisson with wave dissipating concrete blocks.

The transmission coefficient and the wave overtopping rate of the wave power extracting caisson are smaller than those of the sloping top caisson if the crest heights of the caissons are the same. It is said that the sloping top caisson needs to have a crest height of 1.0 $H_{1/3}$ to reduce the wave transmission to a level as low as that by an ordinary caisson with a crest height of 0.6 $H_{1/3}$. Therefore a wave power extracting caisson with a crest height of 1.0 $H_{1/3}$ has a lower wave transmission coefficient than an ordinary caisson with a crest height of 0.6 $H_{1/3}$. The crest height of 1.0 $H_{1/3}$ is relatively high. However the air chamber can be set at a high level if the breakwater crown is high, and this reduces the risk of the water

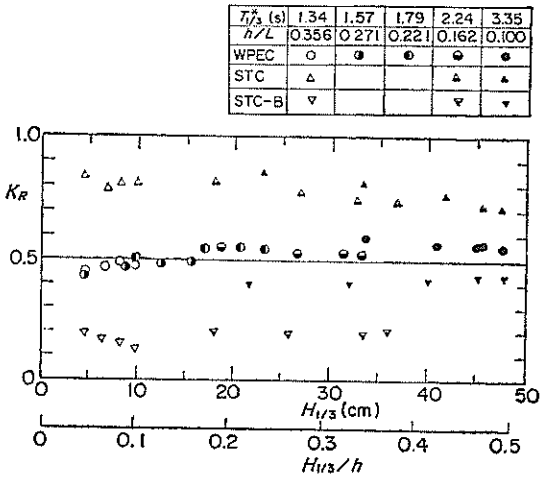

Fig. 41 Reflection Coefficient

intrusion into the turbine room from the air nozzle. The position of the air nozzle in the air chamber should be higher than $0.5\,H_{max}$ above the still water level.

(3) Wave Force

Figure 42 shows the pressure distribution for the design of the air chamber walls of the wave power extracting caisson. Wave-induced positive and negative air pressures act on the air chamber wall. A direct wave pressure also acts on the front wall. Therefore, three phases should be considered in the design as shown in the figure. Although the positive air pressure measured in the model experiments is much larger than that in the figure, the model scale effect of the air compression significantly reduces the pressure in the prototype. This is taken into account to give the pressure distribution in the figure. The model scale effect in the air compression can be predicted theoretically and was already verified by data obtained from field observations[23].

The stability design of the caisson can be performed utilizing the generalized Goda formula. The modification factor λ_1, λ_2, and λ_3 are set to be 1.0, 0 and 1.0 in the design. The effect of the sloping front wall should be considered as described in 3.2.

(4) Field Test of the Wave Power Extracting Caisson at Sakata Port

The Coastal Development Institute of Technology organized a committee to investigate the economical feasibility of a wave power conversion system using a wave power extracting caisson breakwater. About twenty private companies and government organizations joined the committee and the committee concluded that systems with wave power extracting caisson breakwaters are economically feasible and will be constructed in the near future[24]. The First District Port Construction Bureau of the Ministry of Transport has decided to conduct field experiments of the wave power extracting caisson breakwater in Sakata Port from fiscal 1987 to 1991. A prototype wave power extracting caisson breakwater such as shown in Fig. 43 will be installed with a turbine and a generator.

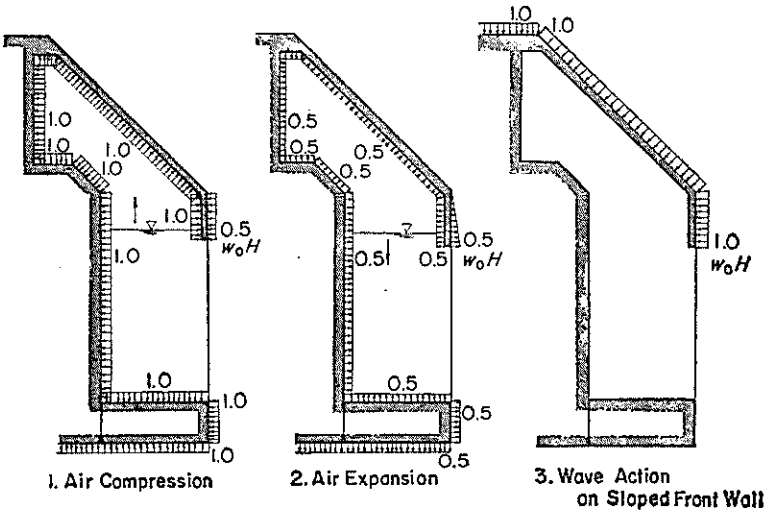

Fig. 42 Pressure Distribution for the Design of Air Chamber Wall

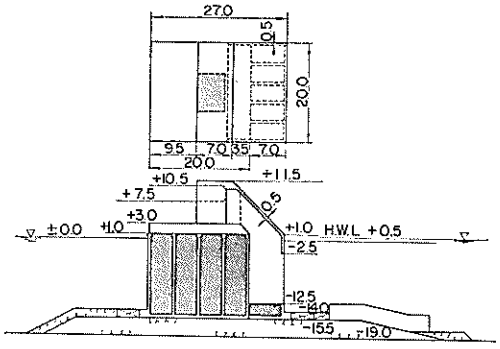

Fig. 43 Sectional View of Wave Power Extracting Caisson at Sakata Port

5. Deep Water Breakwaters

5.1 Basic Shapes of Upright Section of Deep Water Breakwaters

(1) Deep Water Breakwaters in Japan and the Severest Wave Condition

Breakwaters are usually constructed in shallow seas where the water depth is less than 25 m. Due to topographical conditions however, they have been constructed at depths from 30 m to 40 m at several ports as Ofunato, Nagasaki, Kagoshima, and Nase. In addition, the breakwaters under construction at Shimoda Port and Kamaishi Port are to be extended to depths of 42 m and 63 m, respectively.

The largest design wave condition for these deep breakwaters is $T_{1/3}=16.4$ s and $H_{1/3}=8.4$ m at the site of Shimoda Port, although the largest one for all breakwaters in Japan is $T_{1/3}=16.0$ s and $H_{1/3}=12.0$ m at Sakata Port. In this Section, however, the severest wave condition of $T_{1/3}=16.0$ s and $H_{1/3}=14.0$ m in the deep water, which is estimated for the largest typhoon in the past half century, is considered to investigate the optimum shape of the upright section for deep breakwaters. The design wave height at the breakwater site should be determined considering the wave transformation from deep water area to the site. Here, only the transformation due to shoaling and breaking is considered to demonstrate the variation of the wave height with the water depth.

Figure 44 shows the variation of wave heights together with the heights of the upright section of breakwaters at water depths from 10 m to 60 m on the sea bottom slope of 1/100. The significant and the largest wave heights, $H_{1/3}$ and H_{max}, are calculated by Goda's theory[25] of random wave transformation due to shoaling and breaking, and the largest wave height corresponds to $H_{1/250}$. The significant and the largest wave heights are 14.0 m and 25.2 m in the deep water area, respectively. They vary due to shoaling and breaking effects as the propagation towards the shore.

The symbols, h' and l, in the figure indicate the bottom depth and the total height, which are calculated by the following criteria:

$$h'=2.5+\min(0.6h,\ H_{max}) \tag{30}$$

$$l=h'+0.6H_{1/3} \tag{31}$$

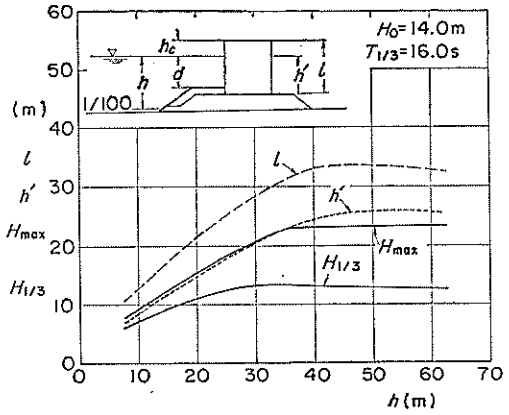

Fig. 44 Variation of Wave Height and Height of Upright Section vs Water Depth

Equation (30) is a condition to avoid the action of impulsive pressures by breaking waves. It is simply assumed that no powerful impulsive pressure acts if the crest depth of the rubble mound foundation including the armour layer is deeper than either $0.6\,h$ or H_{max}. The thickness of the armour layer is assumed to be 2.5 m. The symbol l in Eq. (31) is the total height of the upright section, when the crest height above the still water level is assumed as $0.6\,H_{1/3}$. According to the results, the total height increases with the increasing water depth at first, and becomes almost a constant height of 33 m for deep water of greater than about 40 m. This suggests that a very high upright section must be constructed in deep and rough seas.

(2) Basic Shapes of Upright Section and Design Methods

Three basic shapes of the upright section are compared with the deepwater breakwaters of the rectangular caisson, the trapezoidal caisson, and the cylindrical caisson types as shown in Fig. 45. For all the caissons, the height and the length in the direction of breakwater extension are the same, and are denoted as l and $2R$, where R is the radius of the cylindrical caisson. Other notations in the figure are

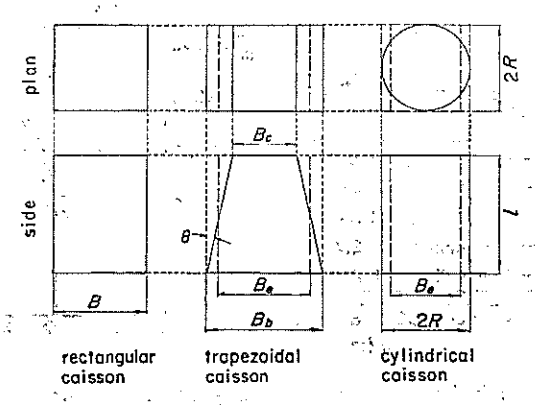

Fig. 45 Basic Shapes of Upright Section

as follows:

B : width of the rectangular caisson

B_c and B_b: top and bottom widths of the trapezoidal caisson

θ : inclination angle of the trapezoidal caisson from the vertical line

B_e : equivalent width of the trapezoidal and the cylindrical caissons to the rectangular caisson with the same volume.

The inclination angle of the trapezoidal caisson, however, is limited to 15 degrees at most due to the constraints in construction works, and the bottom of the cylindrical caisson is assumed to be a rectangular slab with an appropriate thickness.

For these caissons, the design calculations of the stability against the design wave conditions as shown in Fig. 44 are made to determine the size at various water depths. It is assumed that 25% of the total volume of caisson is reinforced concrete, and that the remainder is filled with sand by the required volume. The friction factor is assumed to be 0.6. In addition, the following design criteria are adopted:

a) safety factors against sliding and overturning are 1.2 at least,

b) allowable toe pressure intensity is 60 tf/m².

(3) Calculated Results

Figure 46 shows the bottom and the equivalent widths of caissons. The bottom width governs the size of the rubble mound foundation. At depths deeper than about 30 m, the bottom width is the same for the three caissons, although the bottom width of the cylindrical caisson is larger than those of the others at the shallow depth. The equivalent width shown in Fig. 46 is related to the total volume of the upright section. The equivalent width of the cylindrical caisson is the smallest and the rectangular caisson is the largest.

Figure 47 shows the total side area S which is another aspect of the size of a caisson and is related to the concrete framework. The area of the cylindrical caisson is the minimum and the area of the rectangular caisson is the maximum.

These results of the equivalent width and the total side area suggest that the trapezoidal and the cylindrical caissons can be more economical than rectangular

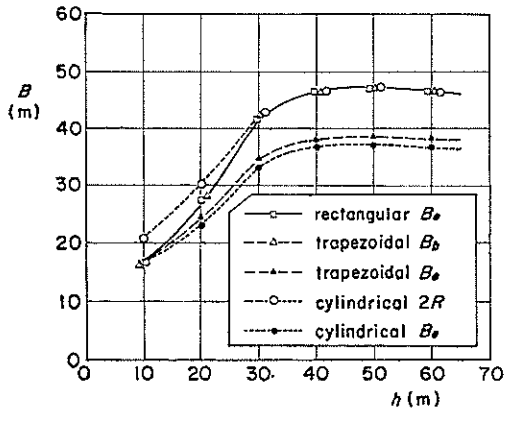

Fig. 46 Bottom and Equivalent Widths of Upright Sections vs Water Depth

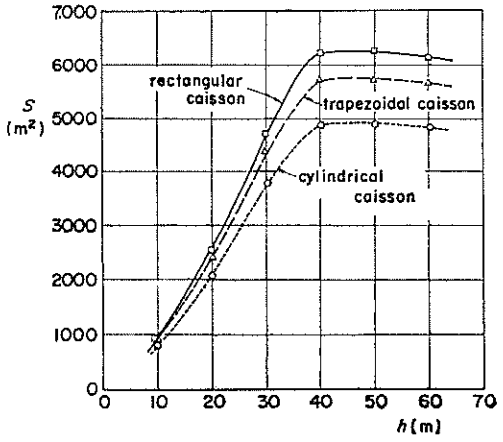

Fig. 47 Total Side Area of Upright Sections vs Water Depth

caissons as the upright sections of deep breakwaters, and the cylindrical caisson, in particular, improves the construction of deep breakwaters.

5.2 Deep Water Breakwaters at Kamaishi Port

(1) Outline of Project

The deepest breakwater in the world is under construction at Kamaishi Port[26]. Figure 48 shows the layout of the breakwater in the Bay of Kamaishi. As seen in this plan, half of the total length of breakwater is located deeper than 50 m and the deepest portion is extended to the depth of 63 m. The breakwater is planned to protect the port area against tsunamis as well as storm waves, and the construction including the preparation works was started in 1978 by the Second District Port Construction Bureau.

Figure 49 shows the proposed cross section at the deep section, where the design wave condition is $T_{1/3}$=12.0 s, $H_{1/3}$=8.0 m at the site. The lower part of the upright section is shaped as a trapezoid to reduce the hydrodynamic pressure during earth-

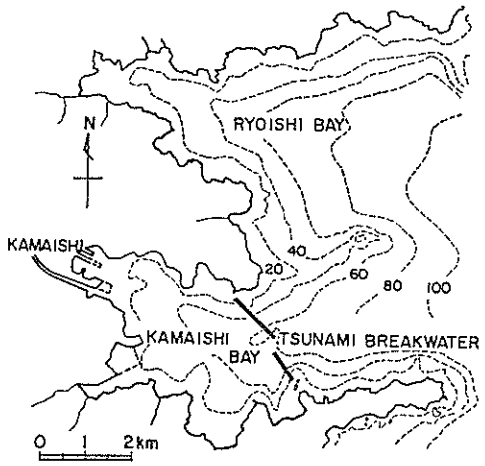

Fig. 48 Plan of Breakwaters at Kamaishi Port

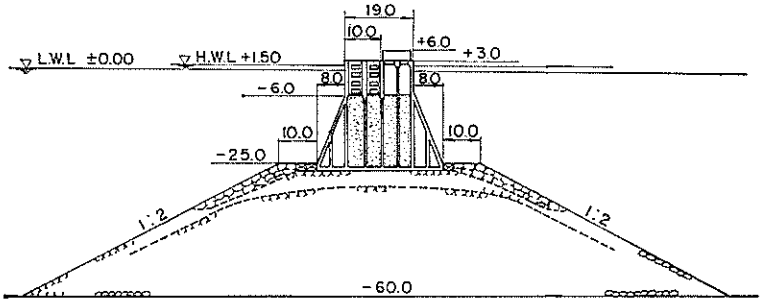

Fig. 49 Proposed Cross Section (Deep Part)

quakes and the upper prat is a wave dissipating type of double horizontal slit walls.

Laboratory experiments have been carried out for the proposed section with a model scale of 1/40[27]. Two alternative sections were tested in order to verify the effectiveness of the wave energy dissipation devices. One was the proposed section and the other was a section with the solid vertical wall in the front. This was realized by placing the rear side of the caisson to face the offshore side. These two sections are called the absorbing type and the reflective type, respectively. The wave forces and the stability against sliding are briefly described on the basis of experimental results in this Section.

(2) Wave Pressure by Irregular Waves

Figure 50 shows the pressure intensity measured at the front wall of the absorbing type. The measuring point is located at a depth of about 28 cm below the still water level. The data are both positive and negative peak values for individual waves. In the figure, the relations calculated by the Goda formula for the positive peak and by the finite standing wave theory of the fourth order approximation for both peaks are also indicated. In the calculations, the upright section is replaced as a vertical wall and the effect of the rubble mound foundation is disregarded for the finite standing wave theory. The measured and calculated results demonstrate that the absolute value of the negative peak intensity is larger than the value of the positive peak intensity. The same tendency is observed in the reflective type. This is a remarkable feature of the standing wave pressures at the relatively deep water.

(3) Results of Sliding Tests

In the experiments, the sliding distance of the upright section was measured for the three different weights of W1, W2 and W3, which are corresponding, respectively, to 0.7, 0.8 and 1.0 times the caisson weight predicted by the design formula. Figures 51 and 52 show the experimental results of the positive and the negative sliding distances for the individual waves, where the positive and negative sliding distances indicate the sliding towards the shore and towards the offshore, respectively. They are expressed in non-dimensional form by H_{cG}, which is the threashold wave height predicted by the Goda formula for the positive sliding. The data are greatly scattered, but the results show that the upright sections are moved in both the direction of the shore and the offshore sides. This is very different from the feasures of shallow water breakwaters which exhibit sliding only in the shore-side

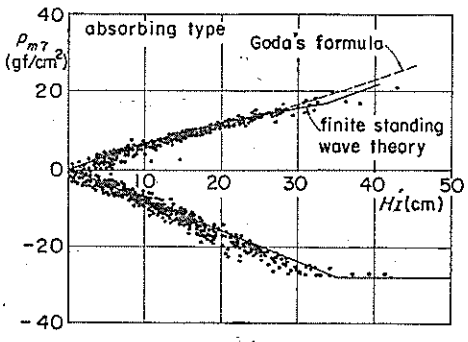

Fig. 50 Positive and Negative Peak Values of Wave Pressure

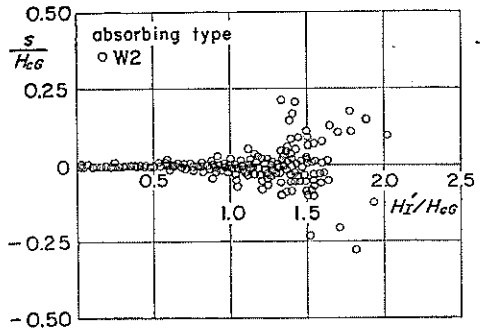

Fig. 51 Sliding Distance by a Wave (Absorbing Type)

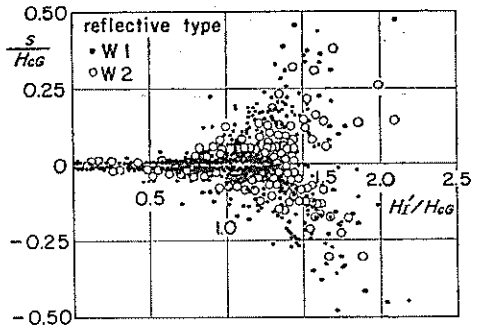

Fig. 52 Sliding Distance by a Wave (Reflective Type)

direction.

The sliding distance of the absorbing type is generally less than that of the reflective type, especially in the positive direction. The reason is that the downward wave force acts at the wave chamber as well as the horizontal wave force decreases slightly. No sliding has been observed for the model caisson of the absorbing type of which the weight was equal to or greater than the design value. It can be said therefore that the absorbing type is more stable against sliding than the reflective type.

5.3 Dual Cylinder Caisson Breakwaters under Development

(1) Structure of Dual Cylinder Caisson

A deepwater breakwater using a cylindrical caisson is being studied in laboratory experiments[28]. The structure tested in the experiments so far is a caisson consisting of dual vertical cylinders fixed on a rectangular base caisson as shown in Fig. 53. The outer cylinder is perforated along the upper one third of the total height. The space between the outer and inner cylinders forms a doughnut shape wave chamber. The upper part of the outer cylinder can be divided into the fore and the rear portions, and different perforation rates can be adopted to them, and denoted as ε_f and ε_r, respectively. A caisson with an extreme value of $\varepsilon_r=0$ is called a wave dissipating type, while a caisson with the perforated rear portion is called the permeable type. In the experiments, the caisson is placed directly on a horizontal bottom at the water depth $h=125$ cm. The outer and the inner diameters of the dual cylinders are 98 cm and 50 cm, respectively, and the height of the base caisson, common for both sections, is 50 cm.

(2) Wave Dissipating Capability

Figure 54 shows the energy dissipation rate defined by the following equation:

$$K_{LOSS}{}^2=1-K_R{}^2-K_T{}^2 \tag{32}$$

where K_R and K_T are the reflection and the transmission coefficients for the significant wave heights. Various combinations of ε_f and ε_r are tested. Among them, a caisson with $\varepsilon_f=\varepsilon_r=0$ is an impermeable single cylindrical caisson, with an energy dissipation rate of less than 0.2. On the other hand, high energy dissipation is achieved by the permeable type of $\varepsilon_f=0.25$ and $\varepsilon_r=0.10$ and by the wave dissipating type of

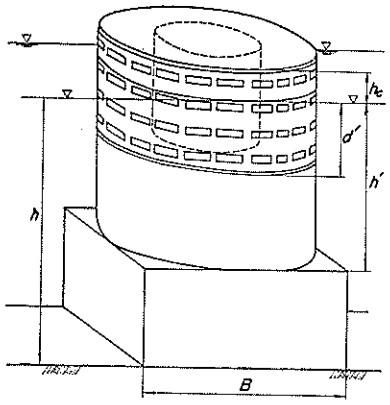

Fig. 53 Dual Cylindrical Caisson

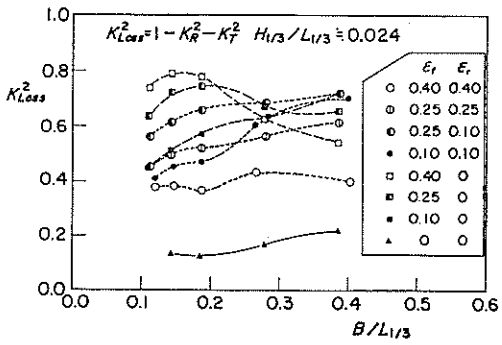

Fig. 54 Energy Dissipation Rate of Dual Cylindrical Caisson

$\varepsilon_f=0.25$ as a whole. Then, the energy dissipation rate is 0.55~0.70 for the permeable type and 0.60~0.75 for the wave dissipating type.

(3) Wave Forces

A method for calculating the wave forces has been proposed for the structures tested. Figure 55 shows the general distribution of the pressure intensity at the phase of the wave crest. The intensity can be calculated by the modification from the wave pressures by the Goda formula for an ordinary vertical wall. The modification factors for various sections of the caisson are presented in Table 1 for two phases around the wave crest. One is defined as phase 1 when the wave pressure at the outer face of the caisson is predominant, and the other is defined as phase 2 when the wave pressure in the wave chamber is predominant.

The negative wave pressure at the wave trough can be obtained appropriately according to the fourth order approximation theory of finite standing waves. The residual water level in the wave chamber, however, must be separately given from the theory as follows:

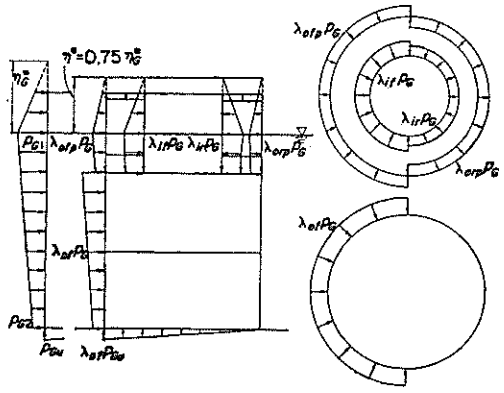

Fig. 55 Distribution of Design Wave Pressure at Wave Crest

Table 1 Modification Factors

modification factor	phase 1	phase 2	
		type 1*	type 2**
λ_{of}	0.90	0.80	0.80
λ_{ofp}	0.65	0.35	0.30
λ_{orp}	0	0.45	0.80
λ_{if}	0.15	0.60	0.75
λ_{ir}	0	0.60	0.75

* permeable type
** wave dissipating type

for the permeable type ($\varepsilon_f=0.25$, $\varepsilon_r=0.10$); $\eta^-=-0.30H$

for the wave dissipating type ($\varepsilon_f=0.25$); $\eta^-=-0.25H$

where η^- is the water level in the wave chamber. The hydrostatic water pressure corresponding to the difference of the water level from the still water must be considered in the wave chamber.

Figure 56 shows the total wave force intensity f_S defined by the following equation:

$$f_S=(F_H\pm\mu F_V)/(h'+h_c) \tag{33}$$

where F_H is the total horizontal force, F_V is the total vertical force, and μ is the friction factor ($=0.6$). The plus and minus signs in the equation correspond to the sign of F_H. The experimental data in the figure are representative values like the maximum, the largest 1/10 mean, the largest 1/3 mean, and the mean of irregular wave forces and are plotted to the corresponding representative wave heights. It is found that the positive total wave forces on the structures of both permeable and dissipating types considerably decrease from the wave force on the impermeable cylindrical caisson ($\varepsilon_f=\varepsilon_r=0$). In particular, the permeable type is predicted to

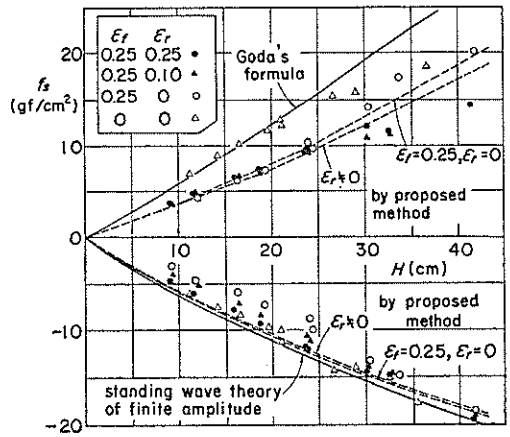

Fig. 56 Total Wave Force Intensity against Sliding

move in the offshore direction at the wave trough rather than in the shore direction at the wave crest. The forces calculated by the proposed method agree well with the experimental forces.

6. Concluding Remarks

Breakwaters are the fundamental harbour facilities in Japan, because the country is surrounded by rough seas. Intensive studies of the wave action on the breakwaters and their structural performances have been carried out during a quarter of century at the PHRI. In this paper, some recent results have been reviewed because most of their results have been reported in Japanese only.

In particular, Chapter 2 described the hydraulic characteristics of the conventional breakwaters including already established formulae. The transformation of irregular waves transmitted behind a breakwater during the propagation still has to be studied theoretically. Another currently exciting subject is the statistical stability of breakwaters. A method for predicting breakwater deformation considering the statistical variability of the stability must be explored.

In Chapters 3 to 5, various new breakwater structures have been introduced. Some of them have already been constructed at the field and are undergoing actual sea tests. Prototype tests for the new breakwater structures introduced in this paper will continue further, and the authors expect that they will be adopted to their full extent in many harbours in the near future. In fact, it has been recently determined by the Third District Port Construction Bureau that dual cylinder caisson breakwaters will be constructed at Shibayama Port.

(*Received on November 18, 1987*)

Acknowledgements

The authors wish to thank Dr. Goda, Director General of the Port and Harbour Research Institute, for his precious comments and critical reviews of the manuscript. Thanks should also be extended to many members of the Breakwaters Laboratory and the Wave Power Laboratory for their cooperation in conducting the studies.

References

1) GODA, Y.: Re-analysis of laboratory data on wave transmission over breakwaters, *Rept. Port and Harbour Res. Inst.*, Vol. 8, No. 3, 1969, pp. 3–18.
2) TANIMOTO, K., and OSATO, M.: Irregular transmitted waves behind mixed type breakwaters covered with wave dissipatng concrete blocks, *Proc. 26th Japanese Conf. Coastal Eng.*, 1979, pp. 309–313 (in Japanese).
3) GODA, Y.: A new method of wave pressure calculation for the design of composite breakwaters, *Rept. Port and Harbour Res. Inst.*, Vol. 12, No. 3, 1973, pp. 31–70 (in Japanese), or *Proc. 14th Coastal Eng. Conf., ASCE*, 1974, pp. 1702–1720.
4) TANIMOTO, K., TAKAHASHI, S., and KITATANI, T.: Experimental study of impact breaking wave forces on a vertical-wall caisson of composite breakwater, *Rept. Port and Harbour Res. Inst.*, Vol. 20, No. 2, 1981, pp. 3–39 (in Japanese).
5) TAKIMOTO, K., TAKAHASHI, S., and MYOSE, K.: Experimental study of random wave forces on upright section of breakwaters, *Rept. Port and Harbour Res. Inst.*, Vol. 23, No. 3, 1984, pp. 47–99 (in Japanese).

6) HUDSON, R. Y.: Laboratory investigation of rubble mound breakwaters, *J. Waterways and Harbors Div., Proc. ASCE*, Vol. 85, No. 31, 1959, pp. 93–121.

7) TANIMOTO, K., YAGYU, T., MURANAGA, T., SHIBATA, K., and GODA, Y.: Stability of armour units for foundation mounds of composite breakwaters by irregular wave tests, *Rept. Port and Harbour Res. Inst.*, Vol. 21, No. 3, 1982, pp. 3–42 (in Japanese).

8) TANIMOTO, K., YAGYU, T., and GODA, Y.: Irregular wave tests for composite breakwater foundation, *Proc. 18th Conf. Coastal Eng., ASCE*, 1982, pp. 2144–2163.

9) TANIMOTO, K., HARANAKA, S., and YAMAZAKI, K.: Experimental study on the stability of wave dissipating concrete blocks against irregular waves, *Rept. Port and Harbour Res. Inst.*, Vol. 24, No. 2, 1985, pp. 85–120 (in Japanese).

10) MORIHIRA, M., and KUNITA, O.: Model experiments on hydraulic characteristics of sloped-wall breakwater, *Proc. 26th Japanese Conf. Coastal Eng.*, 1979, pp. 295–288 (in Japanese).

11) TANIMOTO, K., and KIMURA, K.: A hydraulic experimental study on trapezoidal caisson breakwaters, *Tech. Note Port and Harbour Res. Inst.* No. 528, 1985, 28p. (in Japanese).

12) GOULLET, M.: Sur certains mouvements périodiques de la mer au voisinage d'une paroi oblique ou courbe, *Annales des ponts et chaussées*, 1937 IV, pp. 476–537.

13) TANIMOTO, K., HARANAKA, S., TOMIDA, E., MURANAGA, T., and SUZUMURA, S.: A hydraulic experimental study on multi-cellular caisson breakwaters, *Rept. Port and Harbour Res. Inst.*, Vol. 20, No. 2, 1981, pp. 41–74 (in Japanese).

14) TANIMOTO, K., OKUMURA, T., NAMERIKAWA, N., HASHIZUME, F., and ISHIMARU, Y.: Development of semi-circular breakwaters, *Proc. Civil Eng. in the Ocean*, Vol. 3, 1987, pp. 7–12 (in Japanese).

15) JARLAN, G. E.: A perforated vertical wall breakwater, *The Dock and Harbour Authority*, Vol. 41, No. 488, 1961, pp. 394–398.

16) TANIMOTO, K., HARANAKA, S., TOMIDA, E., and SUZUMURA, S.: A hydraulic experimental study on curved slit caisson breakwaters, *Rept. Port and Harbour Res. Inst.*, Vol. 19, No. 4, 1984, pp. 3–53 (in Japanese).

17) OJIMA, R., GODA, Y., and SUZUMURA, S.: Analysis of pneumatic-type wave power extractors utilizing caisson breakwaters, A study on development of wave power (1st Rept.), *Rept. Port and Harbour Res. Inst.*, Vol. 22, No. 3, 1983, pp. 125–158 (in Japanese), or OJIMA, R., SUZUMURA, S. and GODA, Y.: Theory and experiments on extractable wave power by an oscillating water-column type breakwater caisson, *Coastal Eng. Japan*, Vol. 27, 1984, pp. 315–326.

18) OJIMA, R. and SUZUMURA, S.: Wave forces on a pneumatic type wave power extractors utilizing caisson breakwaters, A study on development of wave power (2nd Rept.), *Rept. Port and Harbour Res. Inst.*, Vol. 23, No. 1, 1984, pp. 54–81 (in Japanese).

19) TAKAHASHI, S. OJIMA, R., and SUZUMURA, S.: Air power of pneumatic-type wave power extractors due to irregular wave actions, A study on development of wave power (3rd Rept.), *Rept. Port and Harbour Res. Inst.*, Vol. 24, No. 1, 1985, pp. 3–41.

20) TAKAHASHI, S., SUZUMURA, S., and MYOSE, K.: Turbine power of pneumatic-type wave power extractors utilizing caisson breakwaters, A study on development of wave power (4th Rept.), *Rept. Port and Harbour Res. Inst.*, Vol. 24, No. 2, 1985, pp. 205–238 (in Japanese), or Turbine power by wave power extraction system with vertical breakwaters, *Proc. 5th OMAE Conf.*, 1986, pp. 553–559.

21) TAKAHASHI, S., MYOSE, K., and TANAKA, S.: Variation of wave power extraction due to incident angle and directional wave spreading, A study on development of wave power (5th Rept.), *Rept. Port and Harbour Res. Inst.*, Vol. 26, No. 1, 1987,

pp. 3–39.

22) TAKAHASHI, S., ADACHI, T., and TANAKA, S.: Electric power generation by a large-scale model of pneumatic-type wave power converter, A study on development of wave power (6th Rept.), *Rept. Port and Harbour Res. Inst.*, Vol. 26, No. 3, 1987, pp. 3–35 (in Japanese).

23) TAKAHASHI, S., and TANIMOTO, K.: Uplift forces on a ceiling slab of wave dissipating caisson with permeable front wall (2nd Rept.),—Field data analysis—, *Rept. Port and Harbour Res. Inst.*, Vol. 23, No. 2, 1984, pp. 3–25 (in Japanese), or Uplift forces due to compression of enclosed air layer and their similitude law, *Coastal Eng. Japan*, Vol. 28, pp. 191–206, 1985.

24) Coastal Development Institute of Technology: Report of the comprehensive study on wave energy utilization, 1987, 697p. (in Japanese).

25) GODA, Y.: Irregular wave deformation in the surf zone, *Coastal Eng. Japan*, Vol. 18, 1975, pp. 13–26.

26) OBORI, K., KOTANI, H., and KUME, H.: Technical investigation on the design of Kamaishi bay mouth breakwater, *Proc. 10th Symp. Civil Eng. in the Ocean*, 1995, pp. 45–50 (in Japanese).

27) TANIMOTO, K., KIMURA, K., and MIYAZAKI, K.: Study on stability of deep water breakwater against waves (1st Rept.),—Wave forces on upright section of trapezoidal shape and its stability against sliding—, *Rept. Port and Harbour Res. Inst.*, Vol. 27, No. 1, 1988, pp. 3–29 (in Japanese).

28) TANIMOTO, K., KATAOKA, S., HARANAKA, S., SUZUKI, S., SHIMOSAKO, K., and MIYAZAKI, K.: Hydraulic characteristics and design wave forces of double-cylindrical caisson, —A study on development of deepwater breakwater (Part 4)—, *Tech. Note Port and Harbour Res. Inst.*, No. 600, 1987, pp. 1–21 (in Japanese).

List of Symbols

B	:	width of upright section
B_M	:	berm width of rubble mound foundation
d	:	crest depth of armour layer of rubble mound foundation
D	:	damage percent of rubble structure, or width of slit member
f	:	force intensity
F_H	:	horizontal wave force
F_V	:	vertical wave force
h	:	water depth from still water level
h'	:	bottom depth of upright section (caisson)
h_c	:	crest height of upright section above still water level
H	:	wave height
H_I	:	incident wave height
H_R	:	reflected wave height
H_T	:	transmitted wave height
H_{T0}	:	transmitted wave height directly behind breakwater
H_{max}	:	largest wave height of irregular waves
$H_{1/3}$	:	significant wave height
H_D	:	representative wave height in design calculation
H_{cG}	:	threshold wave height predicted by generalized Goda formula against sliding
K_D	:	stability coefficient in Hudson's formula
K_R	:	reflection coefficient

K_T : transmission coefficient
K_{T0} : transmission coefficient directly behind breakwater
L : wavelength
$L_{1/3}$: wavelength corresponding to significant wave period
N_s : stability number of armour units
p : wave pressure intensity
s : sliding distance of upright section
S_r : specific gravity of armour unit relative to water
$T_{1/3}$: significant wave period
w_0 : unit weight of water
W : weight of armour unit
γ_r : unit weight of rubble unit
ε : opening ratio of permeable wall
θ : angle of structure slope measured from vertical
λ : modification factor of wave pressure